

T-3530

THE EFFECT OF THE PRESSURE GRADIENT IN THE
WATER-INVADDED REGION ON THE PERFORMANCE
OF WATER-DRIVE GAS RESERVOIRS

**ARTHUR LAKES LIBRARY
COLORADO SCHOOL of MINES
GOLDEN, COLORADO 80401**

by
Wildan Fuadi

ProQuest Number: 10782993

All rights reserved

INFORMATION TO ALL USERS

The quality of this reproduction is dependent upon the quality of the copy submitted.

In the unlikely event that the author did not send a complete manuscript and there are missing pages, these will be noted. Also, if material had to be removed, a note will indicate the deletion.



ProQuest 10782993

Published by ProQuest LLC (2018). Copyright of the Dissertation is held by the Author.

All rights reserved.

This work is protected against unauthorized copying under Title 17, United States Code
Microform Edition © ProQuest LLC.

ProQuest LLC.
789 East Eisenhower Parkway
P.O. Box 1346
Ann Arbor, MI 48106 – 1346

T-3530

A thesis submitted to the Faculty and the Board of Trustees of the Colorado School of Mines in partial fulfillment of the requirements for the degree of Master of Science (Petroleum Engineering).

Golden, Colorado

Date May 16, 1988

Signed: *W Fuadi*
Wildan Fuadi

Approved: *John D. Wright*
Dr. John D. Wright
Thesis Advisor

Golden, Colorado

Date May 23, 1988

Craig W. Van Kirk
Dr. Craig W. Van Kirk
Head of Department of
Petroleum Engineering

ABSTRACT

The effect of the pressure gradient in the water-invaded region on the performance of water-drive gas reservoirs was studied by altering the material balance equation to include the trapped-gas term. This modified material balance equation was originally proposed by Lutes et al. Water influx was calculated by the van Everdingen-Hurst unsteady state method. Using this technique the net water encroachment is calculated for various times and the results are used to adjust the radius of the gas filled portion of reservoir.

The performance of a hypothetical gas reservoir surrounded by a finite aquifer is presented to compare the conventional and modified material balance methods for a variety of conditions.

The results indicate that, in many cases, the performance of a gas reservoir experiencing water influx is significantly affected by the presence of a pressure gradient in the water-invaded region.

TABLE OF CONTENTS

	<u>Page</u>
ABSTRACT	iii
TABLES AND FIGURES	v
ACKNOWLEDGMENTS	ix
INTRODUCTION	1
CONCLUSIONS	3
LITERATURE REVIEW	5
METHODOLOGY	11
THEORETICAL DERIVATION	11
COMPUTER PROGRAM	22
CALCULATION OF CASES	27
ANALYSIS AND DISCUSSION OF THE RESULTS	29
REFERENCES	38
APPENDIXES	
A SAMPLE CALCULATIONS	74
B PROGRAM LISTING	81

TABLES AND FIGURES

<u>Table</u>	<u>Page</u>
1 Hypothetical Gas Reservoir Aquifer Properties	72
B-1. Performance Prediction without the Gradient Effect	92
B-2. Performance Prediction with the Gradient Effect	93
<u>Figure</u>	<u>Page</u>
1. Schematic of Simplified Radial Flow Model and Saturation Profiles for a Water-Drive Gas Reservoir	41
2. Ultimate Gas Recovery Predictions for Depletion and Water-Drive Gas Reservoirs	42
3. Simplified Flow Diagram of the Calculation Procedure for Performance Predictions of Water-Drive Gas Reservoirs without the Gradient Effect	43
4. Simplified Flow Diagram of the Calculation Procedure for Performance Predictions of Water-Drive Gas Reservoirs with the Gradient Effect	44
5. Effect of Pressure Gradient in the Water-Invaded Region on Pressure Performance for the Base Case with $R_a/R_g = 2.0$	45
6. Effect of Pressure Gradient in the Water-Invaded Region on Pressure Performance for the Base Case with $R_a/R_g = 4.0$	46
7. Effect of Pressure Gradient in the Water-Invaded Region on Pressure Performance for the Base Case with $R_a/R_g = 6.0$	47

<u>Figure</u>	<u>Page</u>
8. Effect of Pressure Gradient in the Water-Invaded Region on Pressure Performance for the Base Case with $R_a/R_g = 10.0$	48
9. Effect of Pressure Gradient in the Water-Invaded Region on P/Z Performance for the Base Case with $R_a/R_g = 2.0$	49
10. Effect of Pressure Gradient in the Water-Invaded Region on P/Z Performance for the Base Case with $R_a/R_g = 4.0$	50
11. Effect of Pressure Gradient in the Water-Invaded Region on P/Z Performance for the Base Case with $R_a/R_g = 6.0$	51
12. Effect of Pressure Gradient in the Water-Invaded Region on P/Z Performance for the Base Case with $R_a/R_g = 10.0$	52
13. Effect of Pressure Gradient in the Water-Invaded Region on Pressure Performance for the Base Case with $Q_g = 10$ MMCFD	53
14. Effect of Pressure Gradient in the Water-Invaded Region on Pressure Performance for the Base Case with $Q_g = 50$ MMCFD	54
15. Effect of Pressure Gradient in the Water-Invaded Region on P/Z Performance for the Base Case with $Q_g = 10$ MMCFD	55
16. Effect of Pressure Gradient in the Water-Invaded Region on P/Z Performance for the Base Case with $Q_g = 50$ MMCFD	56
17. Effect of Pressure Gradient in the Water-Invaded Region on Pressure Performance for the Base Case with $K_w = 100$ md	57
18. Effect of Pressure Gradient in the Water-Invaded Region on Pressure Performance for the Base Case with $K_w = 200$ md	58
19. Effect of Pressure Gradient in the Water-Invaded Region on P/Z Performance for the Base Case with $K_w = 100$ md	59

<u>Figure</u>	<u>Page</u>
20. Effect of Pressure Gradient in the Water-Invaded Region on P/Z Performance for the Base Case with $K_w = 200$ md	60
21. Effect of Pressure Gradient in the Water-Invaded Region on Pressure Performance for the Base Case with various Values of S_{gr}	61
22. Effect of Pressure Gradient in the Water-Invaded Region on P/Z Performance for the Base Case with various Values of S_{gr}	62
23. Effect of Pressure Gradient in the Water-Invaded Region on Pressure Performance for the Base Case with various Dip Angles	63
24. Effect of Pressure Gradient in the Water-Invaded Region on P/Z Performance for the Base Case with various Dip Angles	64
25. Effect of Pressure Gradient in the Water-Invaded Region on Pressure Performance for the Base Case with $S_{gr} = 0\%$, and various Dip Angles	65
26. Percent Error in Pressure Prediction Caused by Omission of Pressure Gradient in the Water-Invaded Region for the Base Case with various Values of R_a/R_g	66
27. Percent Error in Pressure Prediction Caused by Omission of Pressure Gradient in the Water-Invaded Region for the Base Case with various Values of Q_g	67
28. Percent Error in Pressure Prediction Caused by Omission of Pressure Gradient in the Water-Invaded Region for the Base Case with various Values of K_w	68
29. Percent Error in Pressure Prediction Caused by Omission of Pressure Gradient in the Water-Invaded Region for the Base Case with various Values of S_{gr}	69
30. Percent Error in Pressure Prediction Caused by Omission of Pressure Gradient in the Water-Invaded Region for the Base Case with various Dip Angles	70

<u>Figure</u>	<u>Page</u>
31. Percent Error in Pressure Prediction Caused by Omission of Pressure Gradient in the Water-Invaded Region for the Base Case with $S_{gr} = 0\%$, and various Dip Angles	71
32. Percent Error in Pressure Prediction Caused by Omission of Pressure Gradient in the Water-Invaded Region for the Base Case with Dip Angle = 0, and various Values of S_{gr}	72
33. Comparison of Pressure Performance Predictions using Three Different Methods: Conventional MBE, Modified MBE, and Numerical Simulator	73

ACKNOWLEDGMENTS

The author wishes to express his grateful appreciation to Professor John D. Wright, thesis advisor, for his valuable suggestions and guidance throughout this study. The author also wishes to express his appreciation to Professor Robert S. Thompson and Professor Donald G. Davis for serving on his committee.

The author also wishes to thank Dr. Hussien Kazemi for contributing his valuable discussion on the subject matter.

The author thanks Huffco Indonesia which made possible his study at Colorado School of Mines.

The author wishes to express his deepest indebtedness and love to his wife, Enny, for her support and encouragement through the time it took to complete this study.

INTRODUCTION

The efficient operation of water-drive gas reservoirs requires that the planning of the development of the reservoir be done soon after its discovery. It is desirable to predict the performance quickly, for this prediction provides a basis for calculating efficient rates of production, determining surface facility requirements, etc.

The importance of the performance predictions is such that forecasts should be made as accurately as possible. Investments must be scheduled in advance and economic calculations depend on accurate forecasts of gas recovery.

Several variations of the material balance equation, differing in the method used to evaluate water influx, are in common use for predicting the performance of water-drive gas reservoirs. However, it appears that most of these methods neglect the effect of the pressure gradient on trapped gas within the water-invaded region. Case studies^{13,18} demonstrate that reservoir performance can be greatly affected by the presence of this gradient.

A modified material balance equation to account for the pressure gradient effect in the water-invaded region was first described by Lutes et al.¹³ in 1977 for radial

water-drive gas reservoirs. The modification made use of the van Everdingen-Hurst¹⁹ unsteady-state material balance equation. A later publication by Wang et al.¹⁸ in 1987 described a similar approach with modifications to include gravity and formation compaction effects, as well as reservoirs with linear geometry.

Although these methods have been used to study of specific field performance, it appears that no one has studied the general case. Therefore, the methods were used to study the differences between the conventional and modified material balance in predicting performance of water-drive gas reservoirs for various conditions.

It is felt that the presentation of the results for a wide variety of conditions will be helpful in visualizing the invaded zone pressure gradient effect on the performance with different permeabilities, production rates, relative size of aquifers, etc.

CONCLUSIONS

Based on this study, the following conclusions appear warranted:

1. The performance of water-drive gas reservoirs will be significantly affected by the presence of a pressure gradient in the water-invaded region. Neglecting the pressure gradient can lead to higher predicted reservoir pressures at abandonment resulting in estimates of gas recovery which are lower than those actually observed.
2. The additional term added to the material balance equation for water-drive gas reservoirs satisfactorily describes the pressure gradient effect.
3. The modified material balance method is easy to use and provides more accurate performance predictions of water-drive gas reservoirs with a relatively small increase in computational difficulty compared to conventional material balance calculations.
4. Residual gas saturation has a major effect on the performance of a gas reservoir experiencing water influx.
5. The error in the performance predictions using the conventional material balance increases as gas

production rate, dip angle, and residual gas saturation increase.

6. The error in the performance predictions using the conventional material balance increases as the relative size of aquifer increases. The relative aquifer size is not the major parameter, indeed the error is almost negligible if the radius of the aquifer is less than 2.0 times the radius of the gas zone.

LITERATURE REVIEW

Several methods for predicting the depletion performance of natural gas reservoirs have been published in the literature. The P/Z versus cumulative gas production (G_p) plot is a commonly accepted method used to obtain original gas in place in normally pressured, volumetric, gas reservoirs. This technique is the straight line graphical solution to general material balance equation.⁵ In an abnormally pressured or water-drive gas reservoirs the plot of P/Z versus cumulative gas production will not generally be linear. The extrapolation of the plot to P/Z of zero yields the apparent gas in place, which may be insignificant error of the true original gas in place.

ABNORMALLY PRESSURED RESERVOIRS

In abnormally pressured reservoirs, the gas compressibility can approach formation compressibility since these reservoirs usually have an initial pressure gradient over 0.85 psi/ft. This makes it necessary to include both formation and water compressibility in the P/Z plots when trying to estimate original gas in place.

Ramagost et al.¹⁵ studied P/Z plots for abnormally

pressured gas reservoirs. The study showed that P/Z curve should be adjusted for rock and water compressibility before extrapolation to the original gas in place in abnormally pressured gas reservoirs. Ignoring rock and water compressibility in the P/Z extrapolation can lead to significant error in the estimated original gas in place.

WATER-DRIVE RESERVOIRS

If the gas reservoir is in contact with an aquifer, the reduction of reservoir pressure will be accompanied by water encroachment. The rate of water influx and, thus, the slope of P/Z curve, depend on the physical properties of the aquifer.

Studies which ignore the Pressure Gradient in the Water-Invaded Region

A number of authors have analyzed the problem of the depletion performance in water-drive gas reservoirs. Neglecting the effect of the pressure gradient in the water-invaded region is one of several assumptions used in their study.

Bruns et al.³, studied the effect of water influx on the P/Z versus cumulative gas production curves. From their study they concluded that it is dangerous to extrapolate the P/Z curve as a straight line without

considering the possibility of water influx.

Shagroni, M.A.¹⁷ studied the effect of formation compressibility, and edge water on gas field performance. From the results of his study he concluded that (1) it is incorrect to extrapolate the early part of the P/Z curves as a straight line to $P/Z = 0.0$ to estimate the initial gas in place without considering the possibility of water influx and the effect of formation compressibility, (2) the sensitivity of the performance curves (P/Z vs. Gp) to formation compressibility increases as the initial reservoir pressure increases, and decreases as the aquifer size increases.

Agarwal et al.¹ used a material balance model to study the effects of water influx on natural gas recovery. On the basis of their calculations for edge water-drive reservoirs, they concluded that recovery depends on (1) the production rate and manner of production, (2) the residual gas saturation in the water-invaded zone, (3) the aquifer properties, (4) the permeability, and (5) the volumetric sweep efficiency of encroaching water zone.

Al-Hashim, H.S.² studied the effect of gas production rate on the performance of partial water-drive gas reservoir. He concluded that gas recovery appeared to be sensitive to the aquifer size, initial reservoir pressure,

and gas production rate. As aquifer size and reservoir pressure increases, ultimate gas recovery decreases. The sensitivity of recovery factor to gas production rate increases in large reservoirs as aquifer size increases. He also stated that a declining production rate should be avoided as much as possible in order to maximize cumulative gas recovery and decrease the producing life of the reservoir.

Studies which include the Pressure Gradient in the Water-Invaded Region

Another water-drive gas reservoir problem more recently presented in the literature^{13,18} concerns the existence of a large pressure gradient in the water-invaded region. Case studies show that the performance of water-drive gas reservoirs can be greatly affected by the presence of this gradient.

Lutes et al.¹³ proposed a modified material balance method to account for the pressure gradient effect in a radial water-drive gas reservoir based on the van Everdingen and Hurst¹⁹ unsteady-state material balance equations. The method has been applied to their study of accelerated blowdown of the Katy V-C gas reservoir which is under strong water-drive. The study showed that reservoir pressure/production performance did not conform to

conventional material balance predictions because of the presence of a substantial pressure gradient in the water-invaded region, the effect of which was not modeled by the conventional material balance. Using the modified material balance equations, it was possible to accurately match the pressure/production performance for the Katy reservoir.

Wang et al.¹⁸ developed a microcomputer program to calculate the gas material balance with water influx. A similar approach to that of Lutes et al. to account for the effect of a large pressure gradient in the water-invaded region was included in their program. In addition, they also included gravity and formation compaction effects, and extended the method to reservoirs with linear geometry. A case study which illustrates the application of the program to a water-drive gas reservoir with a high dip angle showed that the pressure gradient effect is significant in the performance predictions of the reservoir. The study showed that the difference in predicted average reservoir pressure between two runs, with and without the pressure gradient option, was about 742 psi (11.2% of original pressure) at the end of production.

WATER INFLUX MODELS

Estimating the amount of water influx entering a

producing reservoir can be very difficult because aquifer characteristics including pressure, permeability, areal extent, and shape are all usually unknown. Many authors have presented models for estimating water influx such as those of "small pot" as explained by Dake⁸, Schilthuis¹⁶, Hurst¹¹, van Everdingen-Hurst¹⁹, Fetkovitch⁹, and Carter-Tracy⁴. These models have application for different flow geometries (bottom, edge, linear, radial, etc.) and flow regimes, including steady-, modified steady-, pseudosteady-, and steady-state. The method chosen for this study was the van Everdingen-Hurst¹⁹ unsteady-state model.

METHODOLOGY

The methodology section is divided into two parts- the derivation of the modified material balance and a discussion of the computer program used in this study.

THEORETICAL DERIVATION

Since the behaviour of a gas reservoir in communication with an aquifer depends on both the aquifer and the reservoir characteristics, the physical system studied was the combined gas reservoir plus aquifer. In reservoir engineering it is common practice to consider only the total withdrawal of gas from the reservoir regardless of the distribution of pressure in the gas zone and the wells' distribution. In other words, a material balance is made on the hydrocarbon reservoir as a whole.

Gas Material Balance Equation

The general form of the material balance equation for a gas reservoir is:

$$GB_{gi} = (G - G_{pw})B_g + W_e - W_pB_w \quad (1)$$

Where G = original wet gas in place, scf

- B_g = gas formation volume factor at current reservoir pressure, rb/scf
 B_{gi} = gas formation volume factor at initial reservoir pressure, rb/scf
 B_w = water formation volume factor, rb/stb
 W_e = cumulative water influx, bbls
 W_p = cumulative water produced, stb
 G_{pw} = cumulative wet gas produced, scf
 $\quad = G_p + K_C G_C$ (1a)
 G_p = cumulative dry gas produced, scf
 G_C = cumulative condensate produced, stb
 K_C = condensate conversion factor, scf/stb
 $\quad = 132790 \gamma_C / M_{LC}$ (1b)
 γ_C = specific gravity of condensate
 M_{LC} = molecular weight of condensate
 $\quad = 6084 / (^{\circ}\text{API} - 5.9)$ (1c)

The gas formation volume factor can be written as:

$$B_g = \frac{T P_{sc} Z}{5.6146 T_{sc} P} \quad (2)$$

- where Z = gas compressibility factor
 T = reservoir temperature, $^{\circ}\text{R}$.
 P = reservoir pressure, psia

P_{SC} = standard pressure (14.73 psia)

T_{SC} = standard temperature (520 °R)

For a dry gas reservoir, wet gas production (G_{pw}) equals dry gas production (G_p) since condensate production (G_c) equals zero. Therefore, for a dry gas reservoir with no water production, equation (1) becomes:

$$GB_{gi} = (G - G_p)B_g + W_e \quad (3)$$

This equation can be rearranged and expressed in terms of P and Z as:

$$\frac{P}{Z} = \frac{P_i}{Z_i} \left(1 - \frac{G_p}{G} \right) \Bigg/ \left(1 - \frac{W_e}{GB_{gi}} \right) \quad (4)$$

For a radial system the cumulative water influx into the reservoir can be closely approximated using the van Everdingen and Hurst¹⁹ unsteady-state equation

$$W_e(t^{n+1}) = B \sum_{j=0}^n \left\{ (\Delta P_j) W_{eD}(t_D^{n+1} - t_{Dj}) \right\} \quad (5)$$

where

$$B = 1.119 \phi h C_e (R_g)^2 f \quad (6)$$

$$\Delta P_j = \frac{P_{j-1} - P_{j+1}}{2} \quad (7)$$

and

$$t_D = \frac{0.006323 k_w t}{\phi \mu_w C_e (R_g)^2} \quad (8)$$

are functions of time, reservoir geometry, and fluid properties and where :

ϕ = porosity, fraction

h = aquifer thickness, ft

μ_w = viscosity of water, cp

k_w = aquifer permeability, md

t = time, days

f = fraction of perimeter of circle that original gas/water boundary constitutes

C_e = effective compressibility of aquifer, psi^{-1}
 $= C_f + C_w$

C_w = compressibility of water, psi^{-1}

C_f = compressibility of rock, psi^{-1}

R_g = gas reservoir radius, ft

when the gas accumulation is circular, the gas reservoir radius is given by:

$$R_g = \left\{ \frac{5.6146 GB_{gi}}{\pi \phi h (1 - S_{wi})} \right\}^{0.5} \quad (9)$$

where S_{wi} = initial water saturation, fraction.

W_{eD} is dimensionless water influx which is usually determined from a table or graph as a function of dimensionless time (t_D) and the ratio of aquifer to gas reservoir radius (R_a/R_g).

The pressure used in the aquifer equation (5), called P_{rg} , refers to the pressure at the original gas water contact (OGWC). The material balance solution is usually made with an assumption that P_{rg} equals P_{rc} which is the average reservoir pressure in front of the current gas water contact (CGWC). In other words, the effect of the pressure gradient in the water-invaded region is negligible.

Neglecting the presence of pressure gradient in the water-invaded region is a reasonable assumption early in the productive life since only a small amount of influx has occurred. But, as production from the reservoir increases, a substantial pressure gradient may be created in the water-invaded region between the original and the current gas water contact, the effect of which is not modeled by the conventional material balance. Ignoring the effect of

this gradient can cause inaccuracies in the performance predictions such that : (1) the predicted reservoir pressure may be higher than observed pressure, and (2) the predicted gas recovery may be less than observed. Accordingly, as water influx enters into the reservoir, the conventional material balance (equation 3) has to be modified to account for higher pressures in the water-invaded region as described by Lutes et al.¹³ and Wang et al.¹⁸

Figure 1 illustrates the schematic configuration of the reservoir model for modified material balance where:

- R_g = radius of gas reservoir at OGWC, ft
- R_c = radius of gas reservoir at CGWC, ft
- P_{rg} = pressure at R_g at time t , psi
- P_{rc} = pressure at R_c at time t , psi
- P_t = the average pressure in the water-invaded region, psi.

Knowing R_g and having estimated W_e by solving equation (5), the radius of the gas reservoir at the current gas water contact, R_c , can be calculated by:

$$R_c = \left\{ R_g^2 - \frac{5.6146 W_e}{(1 - S_{gr} - S_{wi}) \pi \phi h f} \right\}^{0.5} \quad (10)$$

where S_{gr} = residual gas saturation, fraction
 S_{wi} = initial water saturation, fraction

If Darcy's radial flow equation can be used to describe the pressure distribution in the water-invaded region and the pressure is uniform throughout the uninvaded region of the reservoir, the average reservoir pressure in front of the current gas water contact can be determined by:

$$P_{rc} = P_{rg} - \frac{q_w \mu_w \ln(R_g/R_c)}{0.00708 k_{wg} h} - 0.433 \gamma_w \tan \theta (R_g - R_c) \quad (11)$$

and the average pressure in the water-invaded region can be obtained from the following equation:

$$P_t = P_{rg} - \frac{q_w \mu_w}{0.00708 k_{wg} h} \left\{ 0.5 - \frac{R_c^2 \ln(R_g/R_c)}{R_g^2 - R_c^2} \right\} - 0.433 \gamma_w \tan \theta \left(R_g - \frac{2}{3} \frac{R_g^2 + R_g R_c + R_c^2}{R_g + R_c} \right) \quad (12)$$

where $q_w = \Delta W_e / \Delta t$, res bbl/day
 ΔW_e = net water influx for time step Δt , res bbl
 Δt = time step duration, days

k_{wg} = effective permeability to water at residual
gas saturation, md

γ_w = specific gravity of water

θ = dip angle, degree

The general material balance equation (3) is then modified to account for the invaded region pressure gradient effect as:

$$GB_{gi} = (G - G_p - G_t)B_{gr} + G_t B_{gt} + W_e \quad (13)$$

where G_t = volume of the trapped gas in the invaded
region, scf

$$B_{gt} = B_g \text{ at } P_t$$

$$B_{gr} = B_g \text{ at } P_{rc}$$

and since

$$G_t B_{gt} = \frac{W_e S_{gr}}{1 - S_{gr} - S_{wi}} \quad (14)$$

equation (13) can be rearranged as:

$$GB_{gi} = (G - G_p)B_{gr} + W_e(1 - A) \quad (15)$$

where

$$A = \left(\frac{S_{gr}}{1 - S_{gr} - S_{wi}} \right) \left(\frac{B_{gr} - B_{gt}}{B_{gt}} \right) \quad (16)$$

Arranging equation (15) in terms P and Z results in:

$$\frac{P_{rc}}{Z_{rc}} = \frac{P_i}{Z_i} \left(1 - \frac{G_p}{G} \right) \left/ \left\{ 1 - \frac{W_e(1 - A)}{GB_{gi}} \right\} \right. \quad (17)$$

If the pressure gradient is negligible, P_{rc} and P_{rg} equal P and A will be zero. Then the modified material balance equation will be identical to the conventional material balance equation (4).

Ultimate Gas Recovery Predictions

It has been recognized that for gas reservoirs producing by a natural depletion or partial water-drive, the reservoir may be produced down to atmospheric pressure. However, some abandonment pressure is normally established for commercial production since the production rates decrease as the reservoir pressure approaches atmospheric. The abandonment pressure (P_a) depends on operating line pressure, depth of the reservoir, and the productivity index. The initial gas volume minus the volume at a selected abandonment pressure gives the recoverable gas.

The recovery factor, RF, can then be expressed as:

$$RF = \frac{G_{pa}}{G} = 1 - \frac{P_a Z_i}{Z_a P_i} \quad (18)$$

where G_{pa} is the ultimate gas recovery at P_a .

For gas reservoirs with an active water-drive, pressure decline is not the reason for abandoning the reservoir. The pressure will be wholly or partially maintained by the movement of water into the reservoir as gas is withdrawn and all wells will eventually water out. Therefore, the abandonment pressure may be quite high, sometimes only a few psi below the initial pressure. In such a case the gas recovery may be poor because a substantial amount of the initial gas in place might be trapped in the water-invaded region and in regions not swept by water as residual gas at high pressure.

Agarwal et al.¹ stated that the end point or abandonment condition for a watered out reservoir can be determined based on a material balance which states that the maximum gas recovery is equal to the initial gas in place, less gas trapped as residual gas in the watered out region, less gas in regions not swept by water but unavailable to produce because of water breakthrough into

all existing producing wells.

V_t , the total hydrocarbon pore volume of trapped gas, is given by:

$$V_t = (1 - E_v) + \frac{E_v S_{gr}}{1 - S_{wi}} \quad (19)$$

where E_v is the volumetric sweep efficiency, the gas in place at abandonment can be defined as:

$$G_{paw} = G \left(1 - V_t \frac{P_{aw} Z_i}{Z_{aw} P_i} \right) \quad (20)$$

Equation (20) can be rearranged to:

$$\frac{P_{aw}}{Z_{aw}} = \frac{P_i}{V_t Z_i} \left(1 - \frac{G_{paw}}{G} \right) \quad (21)$$

Equation (21) expresses the end-point (P_{aw}/Z_{aw}) as a linear function of the ultimate gas recovery with intercept G at a zero value of (P_{aw}/Z_{aw}). If (P/Z) versus G_p under water-drive can be estimated by solving Equation (4), the intersection of the performance (P/Z) versus G_p and Equation (21) on the same graph represents the estimated

ultimate gas recovery as presented in Figure 2.

When the pressure gradient in the water-invaded region is such that effect of this gradient becomes significant, the above relation is no longer valid since the reservoir pressure is not equal to the average pressure in the trapped area. At abandonment, where all existing wells have watered out, the cumulative water influx is given by:

$$W_{ea} = GB_{gi} (1 - V_t) \quad (22)$$

Therefore, the ultimate gas recovery (G_{pa}) can be obtained from W_{ea} once the relation of G_p versus W_e is generated by solving equation (15).

COMPUTER PROGRAM

Predicting future gas reservoir performance usually consists of determining how the reservoir pressure will decline for a given production rate. A knowledge of this decline will assist in calculating the recovery factor, consistent with production engineering and economic constraints. The performance of a water-drive gas reservoir can be estimated by solving two basic equations—the reservoir material balance and the water influx equations. Simultaneous solution of these equations by an

iterative process provides the cumulative water influx and reservoir pressure.

Unless a digital computer is used the calculation procedure is quite tedious since it involves an iterative process as well as the van Everdingen and Hurst water influx calculations which include superposition. Therefore, most of the calculations were performed with a high-speed digital computer to make it easier and to permit evaluation of the effect of the pressure gradient on the performance of water-drive gas reservoir under a large variety of conditions. A computer program was written to mechanize the computational and processing aspects of this study.

The study was made to assess the effect of the invaded zone pressure gradient on the performance of a water-drive gas reservoir. The computation of performance can be divided into two main areas: (1) the conventional material balance method, and (2) the modified material balance method. The calculation procedure for each area consists of a sequence of pressure depletion and water influx calculations followed by gas recovery predictions. Examples of calculations for both methods are presented in Appendix A.

A simplified flow diagram of the calculation procedure

designed for the prediction of performance with and without gradient effect is presented in Figures 3 and 4. A listing of the computer programs and samples of output are presented in Appendix B. The sequence of steps in the calculation procedure is as follows:

Conventional Material Balance Method

1. Compute the gas reservoir radius from Equation (9).
2. Select production rate, R_a/R_g , dip angle, aquifer permeability, and residual gas saturation.
3. Calculate G_p for a fixed time increment.
4. Estimate the average reservoir pressure, P .
5. Solve Equation (4) for W_e , and P/Z .
6. Solve Equation (5) for W_e .
7. Compare W_e calculated from step 5 with that calculated from step 6. If the W_e 's are not within a specific tolerance, go to step 4, estimate another P , and repeat the procedure.
8. Solve Equation (21) for P_a/Z_a .
9. Repeat steps 3 through 8 incrementing time until G_p equals G or P_a/Z_a from step 8 is less than P/Z from step 5.
10. Repeat steps 2 through 9 for different values of the key parameters in step 2.

Modified Material Balance Method

1. Compute the original gas reservoir radius, R_g , from Equation (9).
2. Select production rate, R_a/R_g , dip angle, aquifer permeability, and residual gas saturation.
3. Calculate G_p for a fixed time increment.
4. Estimate the pressure, P_{rg} , at the original gas water contact.
5. Solve for water influx, W_e , from Equation (5).
6. Calculate the radius of the uninvaded zone, R_c , by solving Equation (10).
7. Calculate the pressure, P_{rc} , at the invading water front assuming radial flow from Equation (11).
8. Using Equation (12), calculate the average pressure, P_t , in the water-invaded region.
9. Solve Equation (15) for W_e .
10. Compare W_e calculated from step 5 with that calculated from step 9. If the W_e 's are not within a specific tolerance, go to step 4, estimate another P_{rg} , and repeat the procedure.
11. Solve Equation (22) for W_{ea} .
12. Repeat steps 3 through 11 incrementing time until G_p equals G or W_{ea} from step 11 is greater than W_e from step 5.

13. Repeat steps 2 through 12 for different values of the key parameters in step 2.

CALCULATION OF CASES

Hypothetical Gas Reservoir

The method chosen to compare the solutions of the modified and conventional material balance equation (MBE) is a hypothetical gas reservoir surrounded by a finite aquifer. The results for the two methods are presented to show the effect of pressure gradient in the water-invaded region on the performance of water-drive gas reservoir.

The properties of the gas reservoir and aquifer are presented in Table 1. Gas compressibility factor (Z) is calculated as a function of P_r and T_r using a Z -factor subroutine which is a table lookup and interpolation on a table of 400 Z -factors. The relative permeability to water (K_{rw}) at residual gas saturation is calculated as a function of water saturation and can be described as¹⁴:

$$k_{rw} = \left(\frac{S_w - S_{wi}}{1 - S_{wi}} \right)^{0.5} \times (S_w)^3 \quad (22)$$

In order to permit the evaluation of several key parameters so that the effect of the pressure gradient across the reservoir could be investigated, performance was predicted for a range of aquifer permeabilities, production

rates, residual gas saturations, dip angles, and relative sizes of the aquifer. The base case parameters used in this study are as follows:

Aquifer permeability	= 500 md
Residual gas saturation	= 35%
Relative aquifer size	= 10.0
Gas production rate	= 30 MMCFD
Dip angle	= 10 degrees

Numerical Simulation

For comparison to the base case, the pressure performance prediction of the hypothetical reservoir was also modeled with a commercial numerical simulator based on the solution of partial differential equations that describe the reservoir using the finite difference technique. RZ coordinates of 51*1 grid blocks and a fully implicit formulation were used in this study.

ANALYSIS AND DISCUSSION OF THE RESULTS

The results of the calculations for various conditions are presented in Figures 5 through 40. Each curve ends at the abandonment point dictated by the material balance equations (21) and (22) for the conventional and modified material balance methods, respectively. The end point of the curves represents the estimated ultimate gas recovery. In the case of small relative aquifer size where the pressure and P/Z performance are almost identical with that of volumetric depletion, the cut-off point was determined based on the abandonment pressure of 750 psia.

Effect of the Gradient on the Performance Predictions

Figures 5 through 8 illustrate the results of pressure performance predictions for an aquifer permeability of 500 md, a gas production rate of 30 MMCFD, and four different relative sizes of aquifer. The relative aquifer sizes used were 2.0, 4.0, 6.0, and 10.0. The residual gas saturation, and reservoir dip angle were 35%, and 10 degrees, respectively. The P/Z versus cumulative gas production curves for these cases are presented in Figures 9 through 12.

The graphs show that, as the relative size of the

aquifer and the cumulative gas production from the reservoir increase, the modified material balance solutions depart from the conventional material balance solutions. The curves are identical during early production life, but as withdrawal from reservoir increases they differ increasingly. The difference occurs as a result of the presence of a substantial pressure gradient in the water-invaded region.

Figures 13 through 16 illustrate the pressure and P/Z performance predictions when the gas production rates are changed to 10 MMCFD and 50 MMCFD. These cases were run for the largest relative size of aquifer. The other parameters are kept at the base case values. The departure of the pressure performance from that predicted by the conventional material balance equation is most pronounced for the gas producing rate of 50 MMCFD. This is because the larger gas production rates resulted in larger influx rates into the reservoir which causes proportionately larger pressure gradients between the original and the current gas water contact.

Figures 17 through 20 present the performance predictions using 100 md and 200 md aquifer permeabilities and a gas production rate of 30 MMCFD. In these cases as in all previous cases, the performance predictions as

calculated by the modified material balance method increasingly depart from those calculated by the conventional material balance method as cumulative gas production increases.

Another factor which was studied is the residual gas saturation in the water-invaded region. A comparison of the performance predictions for the 500 md case with a gas production rate of 30 MMCFD for various residual gas saturations are shown in Figures 21 and 22. The results show that as residual gas saturation increases the deviation from that conventional material balance method will be significantly larger. This indicates that the residual gas saturation has an important effect upon the presence of the pressure gradient in the water-invaded region. The explanation of this lies in the fact that the relative permeability of water is greatly affected by the value of residual gas saturation. A larger residual gas saturation results lower relative permeability to water. This means that a larger pressure gradient will be created in the water-invaded region which results in a much lower pressure in the uninvaded zone than at the original gas water contact.

A further comparison was made for the same conditions as those shown Figures 21 and 22, except that the dip angle

of the reservoir was varied. The residual gas saturation is 35% for this case. The effects of variation in dip angle on performance predictions are shown in Figures 23 and 24 which exhibit a small increase in the deviation from the conventional material balance method as dip angle increases. This indicates that dip angle is not the dominant factor creating a pressure gradient in the water-invaded region. The increase in pressure gradient in the invaded region as dip angle increases is noticeably less than that caused by increasing residual gas saturation. This is shown in Figure 25 which illustrates the effect of various dip angles for zero residual gas saturation.

Error Analysis on the Performance Predictions

Figures 26 through 32 illustrate the error in pressure predictions which occurs if the performance predictions are made with no regard for the presence of the pressure gradient in the water-invaded region. For all cases, it is clearly shown that as cumulative gas production from the reservoir increases, the percentage error in pressure predictions due to omission of pressure gradient in the water-invaded region increases.

Figure 26 illustrates the percent error in pressure predictions for various relative aquifer sizes. The curves

show that for the relative aquifer size of 2.0, the percentage error due to ignoring the presence of pressure gradient is negligible. However, for a higher relative size of aquifer, ignoring this gradient can lead to an error in predicted pressure as large as 22% at the end of production.

Figure 27 shows the increasing error in pressure predictions for various gas production rates. The error tends to increase as production rate increases. As previously explained, higher production rates create higher pressure gradients across the reservoir. However, the error in pressure predictions is not as sensitive to production rate as it is to the other factors as indicated by the small separation between each of the curves. The high value of error shown by the curves is mainly due to the high residual gas saturation used in this study.

Figure 28 shows the error in pressure predictions for various aquifer permeabilities. It can be seen from the curves that for small to moderate values of aquifer permeability, the error significantly increases as permeability increases. However, for high permeability, the error decreases as permeability increases. The reason is that all aquifers act as if they are infinite for small values of dimensionless time. At later times, boundary

effects are felt and finite aquifer behaviour deviates accordingly.

While the aquifers are infinite acting, larger permeabilities have larger errors because the higher permeability aquifers provide more water influx. When the aquifers are finite acting the larger permeability aquifers have smaller errors because the ΔP across the invaded zone is lower. Different permeability aquifers switch from infinite to finite at different times- higher permeability first. This causes the % error curves to cross over each other in Figure 28.

A factor which has a very important effect on the magnitude of the error in the performance predictions is the residual gas saturation. Figure 29 shows the error in pressure predictions for various residual gas saturations. The curves show that as residual gas saturation increases, the error significantly increases. This indicates that a larger pressure gradient in the water-invaded region will be created as residual gas saturation increases as mentioned earlier.

Figure 30 illustrates the error in pressure predictions for various reservoir dip angles. Although the error increases as dip angle increases which indicates that dip angle is one of the factor creating the presence of the

pressure gradient across the reservoir, the increase in error is noticeably less compared with that caused by increasing residual gas saturation. As a comparison between both parameters, Figure 31 shows the error in pressure predictions for a zero residual gas saturation for various dip angles while Figure 32 shows the error in pressure predictions as residual gas saturation increases for a zero dip angle. It is clearly shown from both figures that dip angle is not the dominant factor in causing a pressure gradient in the water-invaded region.

Comparison with Numerical Simulator

The existence of the invaded zone pressure gradient was confirmed by radial numerical simulations. The comparison between the three methods; conventional MBE, modified MBE, and numerical simulation is presented in Figure 33. The performance predictions were run for aquifer permeability of 500 md, residual gas saturation of 35%, gas production rate of 30 MMCFD, relative aquifer size of 10.0, and dip angle of 10 degrees. The results show that the modified material balance method and the simulator give very comparable pressure performance predictions. This indicates that the modified material balance method satisfactorily describes the pressure gradient effect that

is seen to exist in the water-invaded region.

REFERENCES

1. Agarwal, R.G., Al-Hussainy, R., and Ramey, H.J.: "The Importance of Water Influx in Gas Reservoirs", Jour. Pet. Tech., November 1965, 1336.
2. Al-Hashim, H.S.: "The Effect of Gas Production Rate on The Performance of Partial Water Drive Gas Reservoir", Master of Engineering, Colorado School of Mines, 1979.
3. Bruns, J.R., Fetkovich, M.J., and Meitzen, V.C.: "The Effect of Water Influx on P/Z-Cumulative Gas Production Curves", Jour. Pet. Tech., March 1965, 287.
4. Carter, R.D., and Tracy, G.W.: "An Improved Method for Calculating Water Influx", Trans., AIME (1960) 219, 415.
5. Cole, F.W.: "Reservoir Engineering Manual", Gulf Publishing Company, Houston, Texas (1969), Chapter. 6.
6. Colorado School of Mines Programs Library: 1) Water Influx Subroutine, 2) Z-factor Subroutine, 3) Critical Pressure and Temperature Subroutine.
7. Craft, B.C., and Hawkins, M.F.: "Applied Petroleum Reservoir Engineering", Prentice-Hall, Inc., Englewood Cliffs, N.J., 1959, Chapter 5.
8. Dake, L.P.: "Fundamentals of Reservoir Engineering", Elsevier Scientific Publishing Company, New York (1978), Chapter 9.
9. Fetkovich, M.J.: "A Simplified Approach to Water Influx Calculations-Finite Aquifer Systems", Jour. Pet. Tech., July 1971, 814-828.
10. Frick, T.C.: "Petroleum Production Handbook, Vol. II, Reservoir Engineering", McGraw-Hill, Inc., New York (1962).
11. Hurst, W.: "Water Influx Into a Reservoir and Its Application to the Equation of Volumetric Balance", Trans., AIME, 151, 1943, 57.

12. Klins, M.A., Bouchard, A.J., and Cable, C.L.: "A Polynomial Approach to the van Everdingen-Hurst Dimensionless Variables for Water Encroachment", Soc. Pet. Eng. Reservoir Engineering, February 1988, 320.
13. Lutes, J.L., Chiang, C.P., Rossen, R.H., and Brady, M.M.: "Accelerated Blowdown of a Strong Water Drive Gas Reservoir", Jour. Pet. Tech., December 1977, 1533.
14. Pirson, S. J.: "Handbook of Well Log Analysis : For Oil and Gas Formation Evaluation", Prentice-Hall, Englewood Cliffs, New York, 1963.
15. Ramagost B. P. and Farshad, F. F.: "P/Z Abnormally Pressured Gas Reservoirs", paper SPE 10125, presented at the 1981 SPE Annual Technical Conference and Exhibition, San Antonio, Oct. 1981.
16. Schilthuis, R. J.: "Active Oil and Reservoir Energy", Trans, AIME, 118:37.
17. Shagrioni, M.A.: "Effect of Formation Compressibility and Edge Water Drive on Gas Field Performance", Master of Engineering, Colorado School of Mines, 1977.
18. Wang, B. and Teasdale, T.S.: "GASWAT-PC: A Microcomputer Program for Gas Material Balance With Water Influx", SPE 16484, 1987.
19. Van Everdingen, A.F., and Hurst, W.: "The Application of the Laplace Transformation to Flow Problems in Reservoir", Trans., AIME (1949) 186, 305.
20. Van Everdingen, A.F., Timmerman, E.H., and McMahon, J.J.: "Application of the Material Balance Equation To A Partial Water Drive Reservoir", Trans., AIME (1953), 187, 51.

TABLE 1

Hypothetical Gas Reservoir and Aquifer Properties

1. Rock and fluid properties:
 - a. Aquifer permeability
 - = 1 md
 - = 10 md
 - = 100 md
 - = 200 md
 - = 500 md
 - = 1000 md
 - b. Porosity = 0.25
 - c. Water viscosity = 0.7 cp
 - d. Gas specific gravity = 0.65
 - e. Water specific gravity = 1.02
 - f. Formation compressibility = 5×10^{-6} psi
 - g. Water compressibility = 3×10^{-6} psi
 - h. Initial water saturation = 0.25
 - i. Residual gas saturation in the water-invaded region
 - = 0%
 - = 25%
 - = 35%
 - = 45%
2. Reservoir and aquifer conditions:
 - a. Reservoir thickness = 30 ft
 - b. Initial reservoir pressure = 5000 psia
 - c. Angle subtended by the reservoir circumference = 360 degrees

TABLE 1 Cont'd

d. Relative size of the aquifer R_a/R_g	= 2.0 = 4.0 = 6.0 = 10.0
e. Dip angle	= 0 degrees = 10 degrees = 20 degrees = 30 degrees
f. Initial gas in place	= 100 BCF
g. Production rate	= 10 MMSCF/D = 20 MMSCF/D = 30 MMSCF/D = 40 MMSCF/D = 50 MMSCF/D
h. Volumetric sweep efficiency	= 0.85
i. Reservoir temperature	= 675 °R
k. Reference temperature	= 520 °R
l. Reference pressure	= 14.73 psia
m. Abandonment pressure	= 750 psia

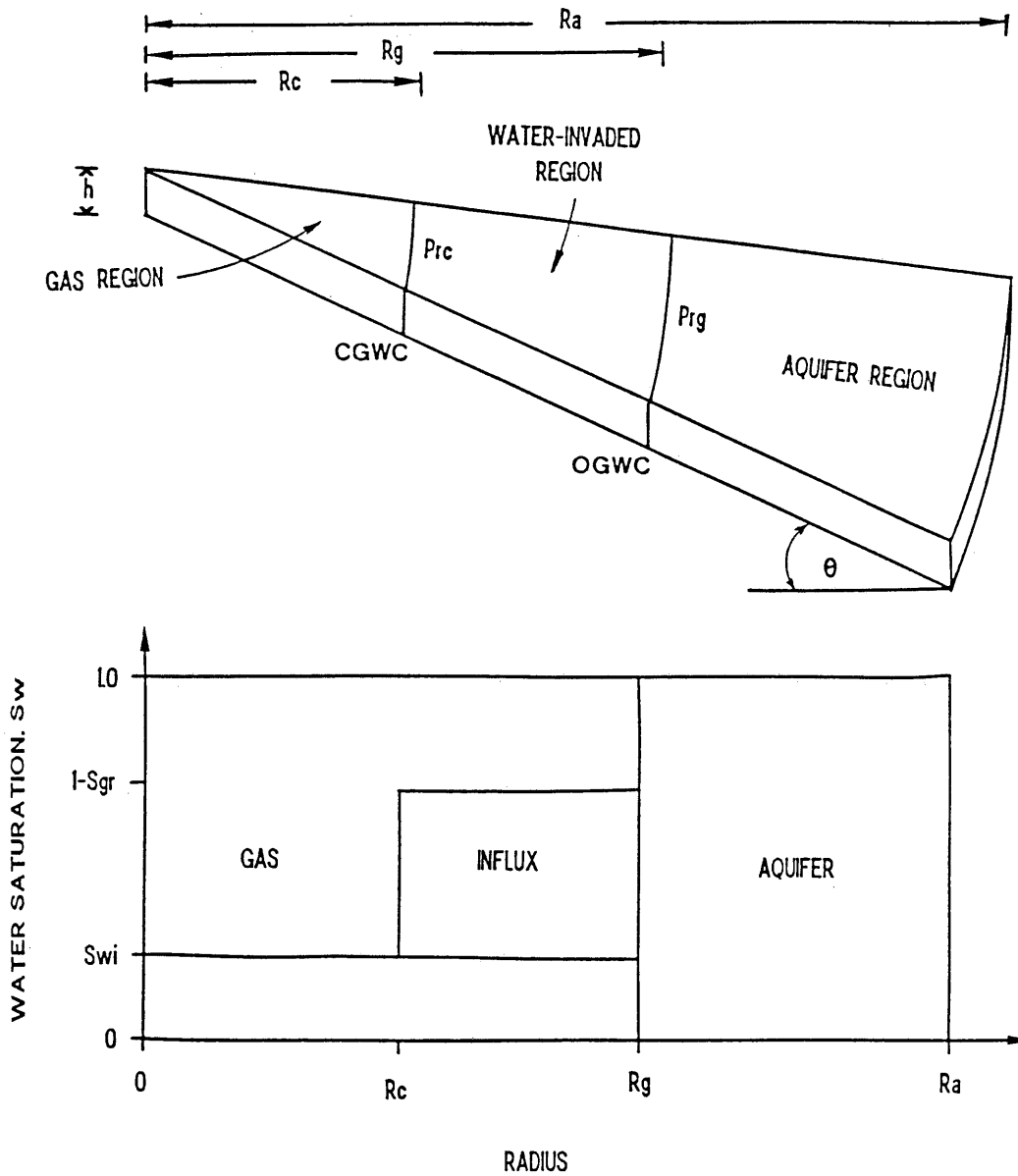


Figure 1. Schematic of Simplified Radial Flow Model and Saturation Profiles for a Water-Drive Gas Reservoir. (After Wang et al.¹⁸)

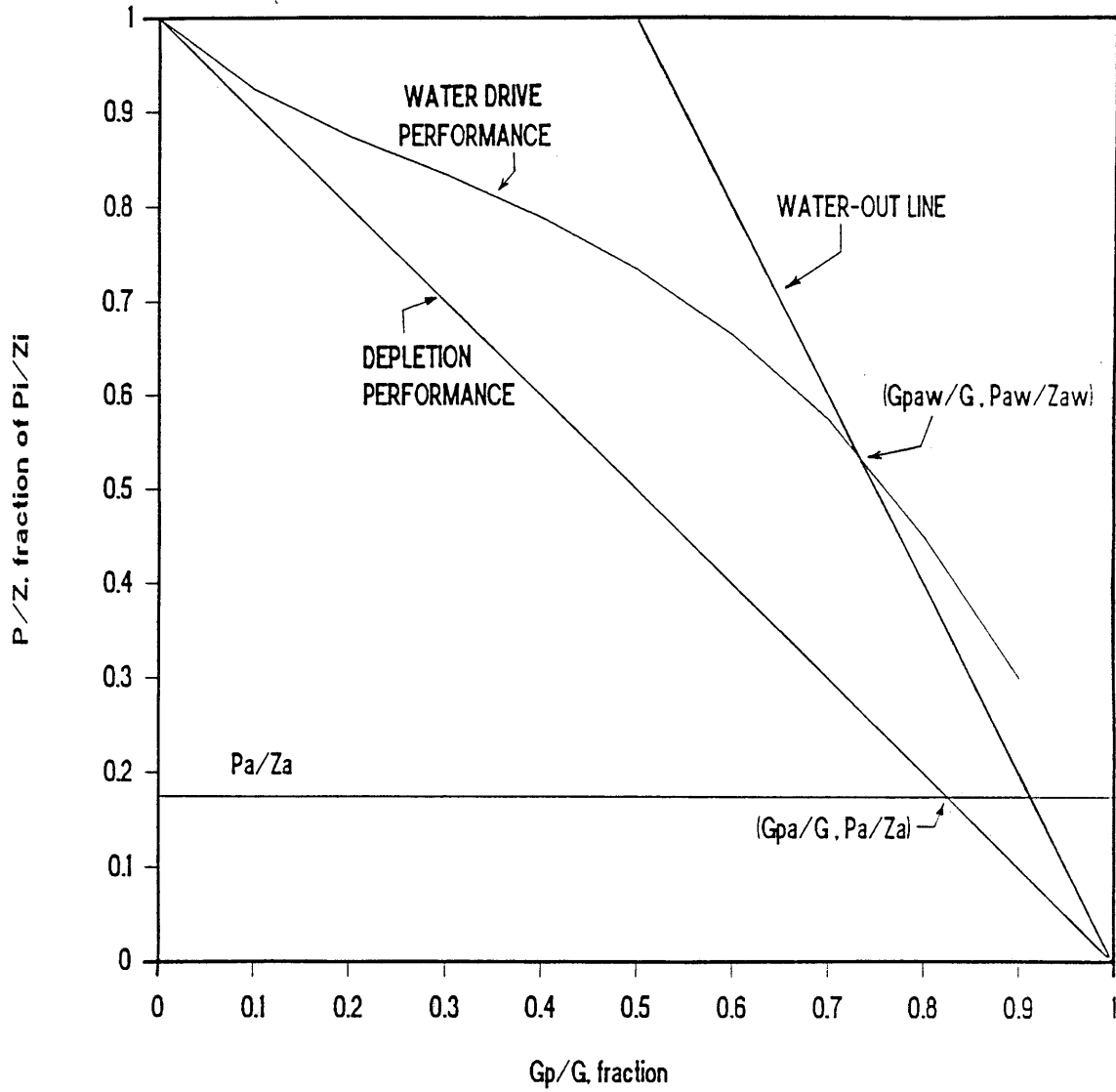


Figure 2. Ultimate Gas Recovery Predictions for Depletion and Water-Drive Gas Reservoirs. (After Wang et al.¹⁸)

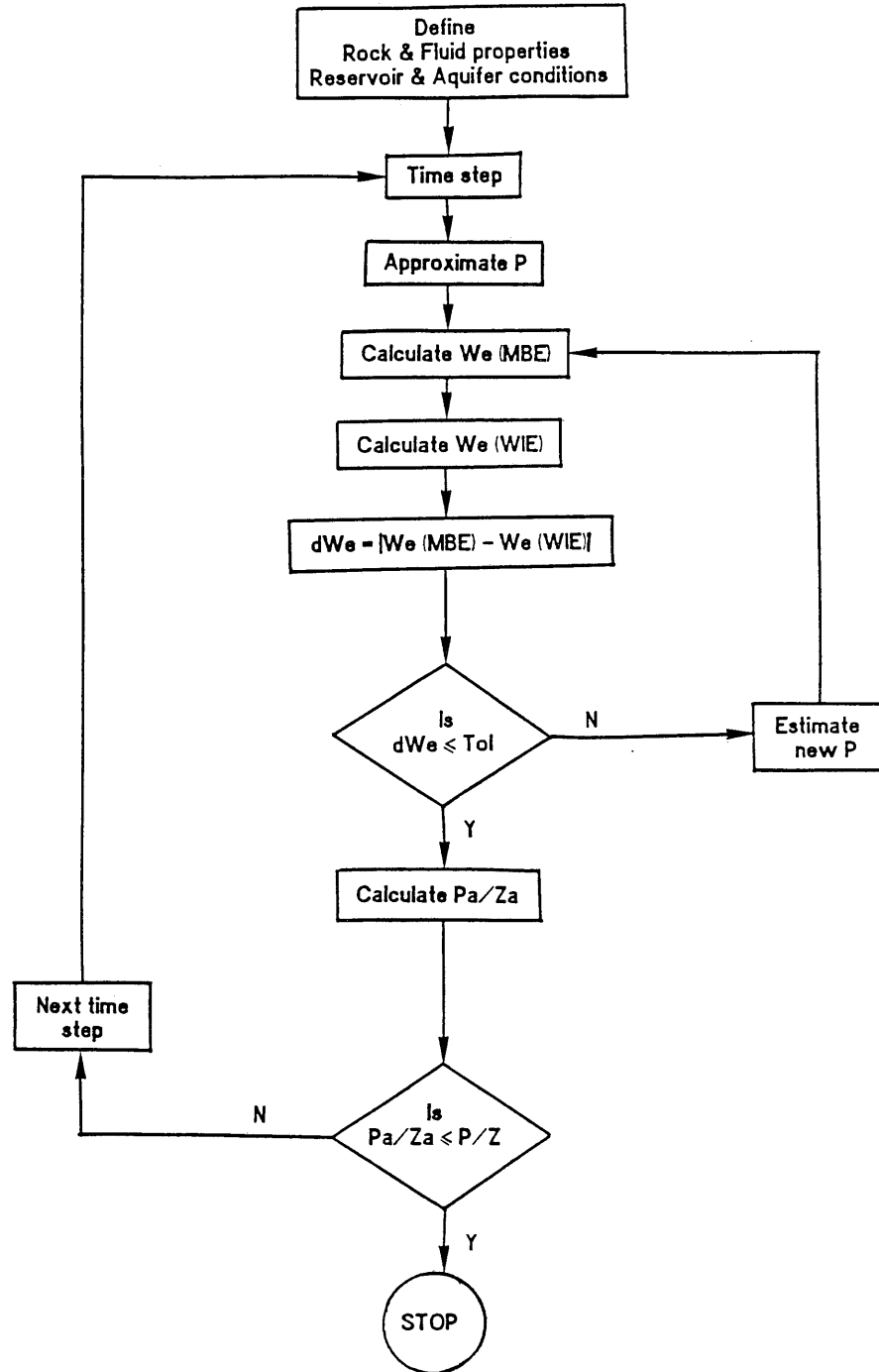


Figure 3. Simplified Flow Diagram of the Calculation Procedure for Performance Predictions of Water-Drive Gas Reservoirs without the Gradient effect.

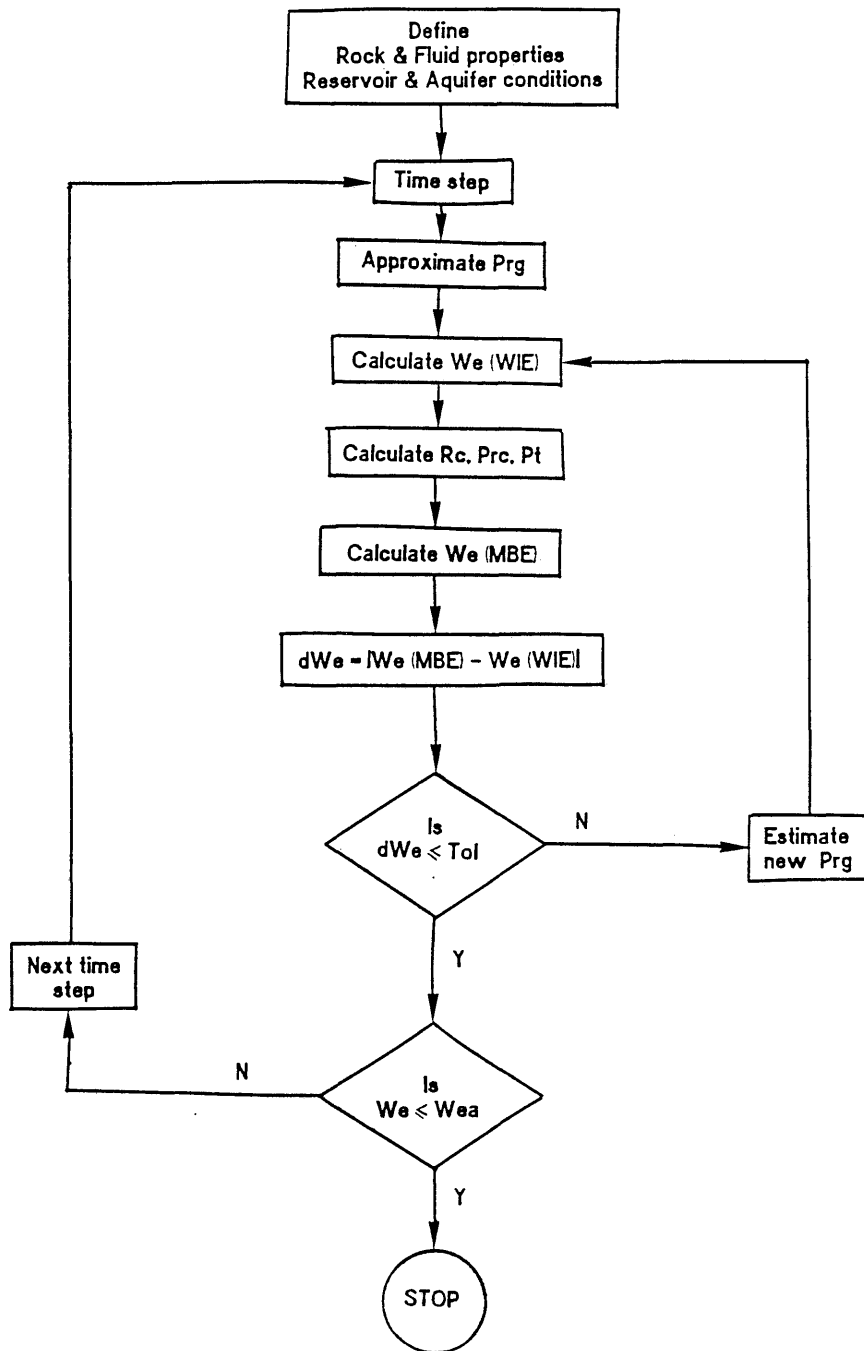


Figure 4. Simplified Flow Diagram of the Calculation Procedure for Performance Predictions of Water-Drive Gas Reservoirs with the Gradient effect.

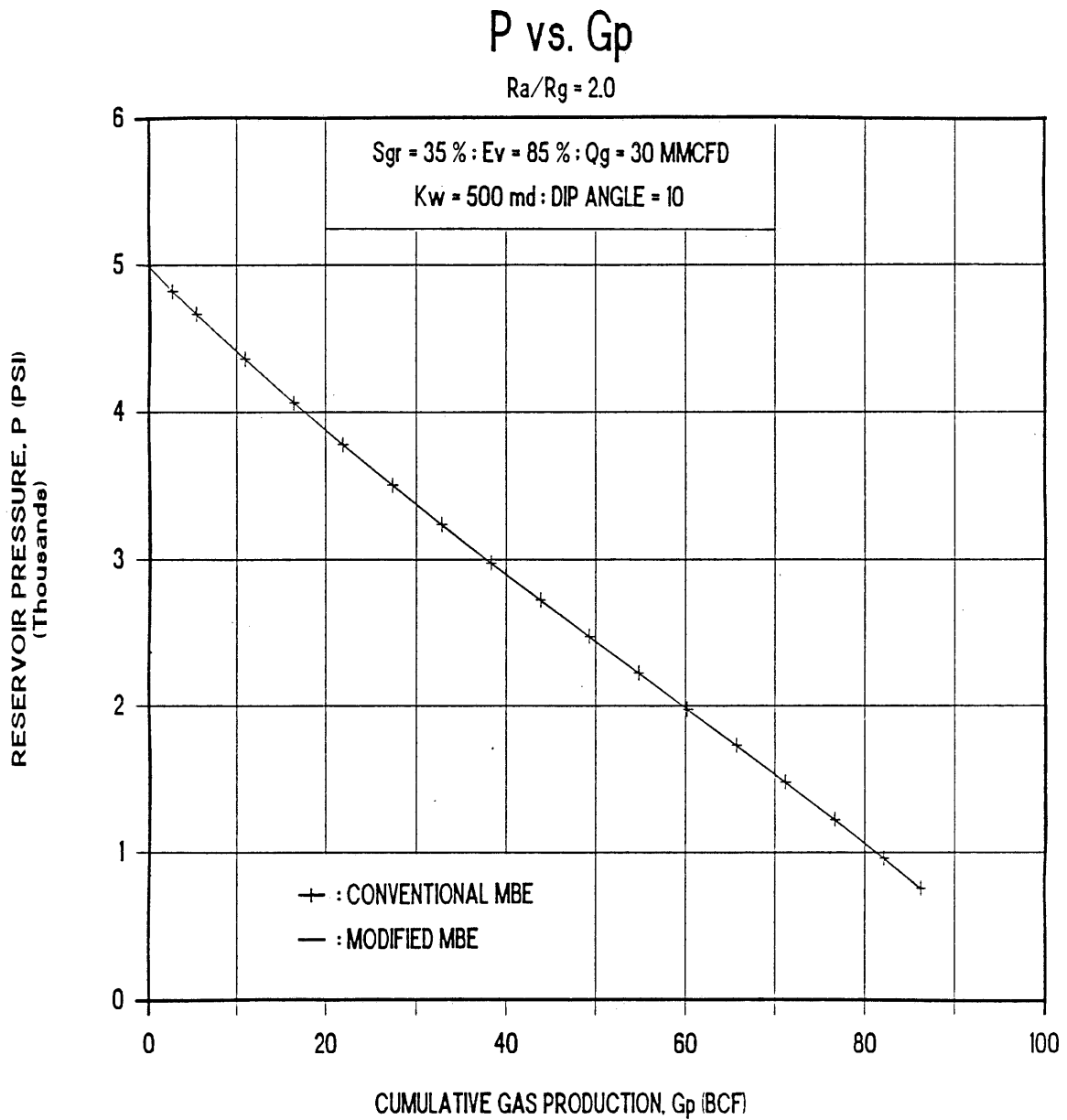


Figure 5. Effect of Pressure Gradient in the Water-Invaded Region on Pressure Performance for the Base Case with $R_a/R_g = 2.0$.

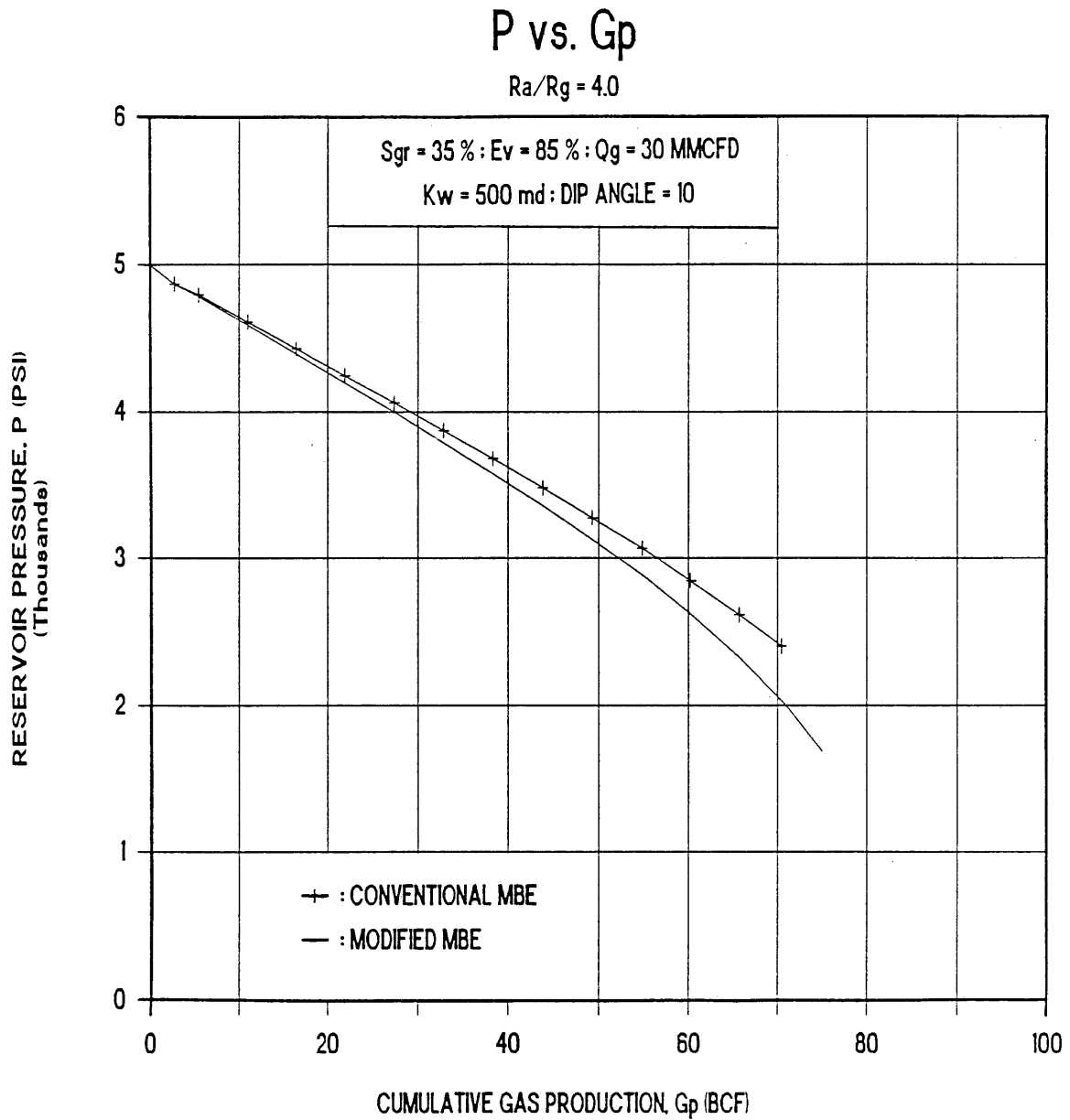


Figure 6. Effect of Pressure Gradient in the Water-Invaded Region on Pressure Performance for the Base Case with $R_a/R_g = 4.0$.

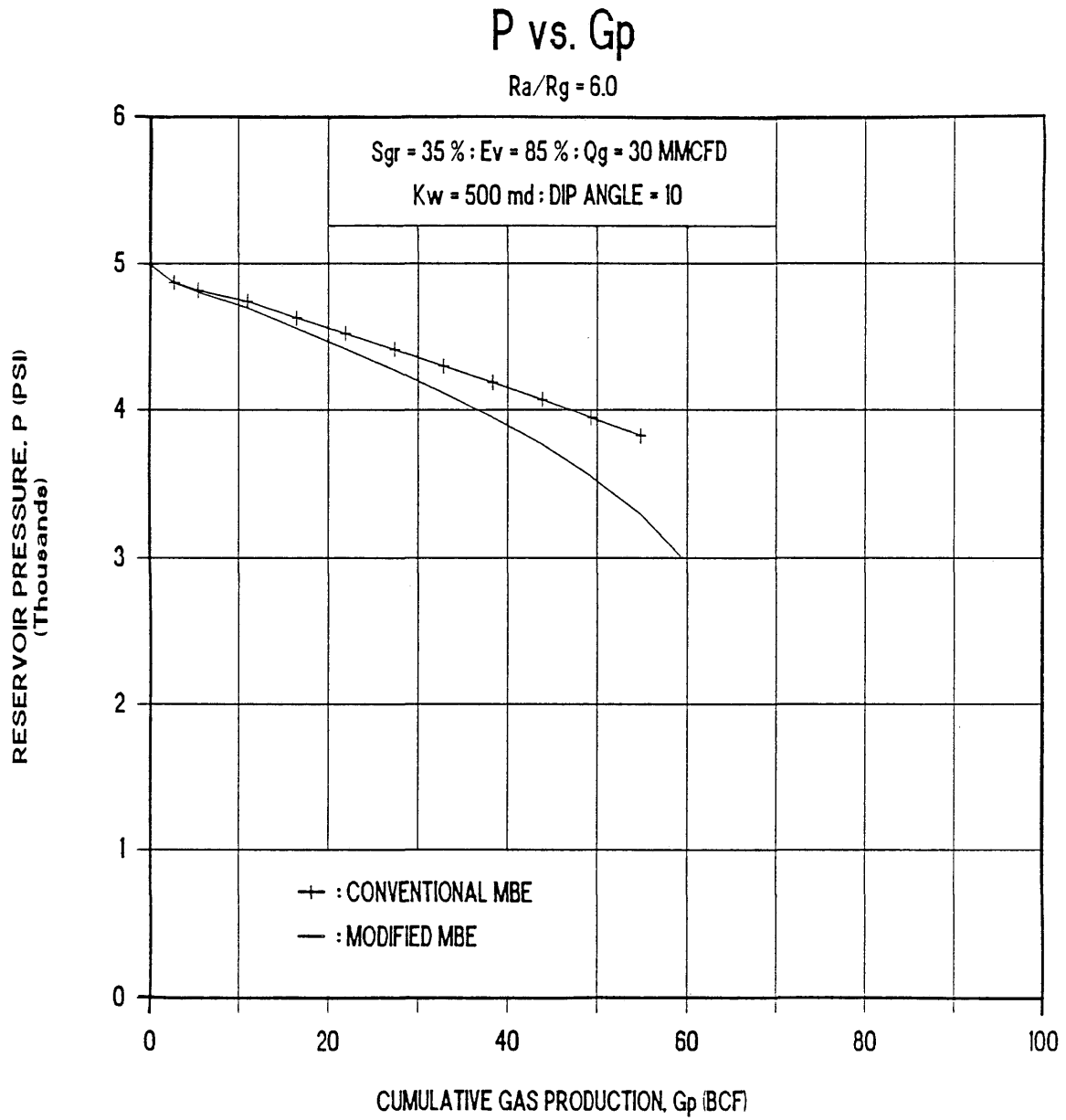


Figure 7. Effect of Pressure Gradient in the Water-Invaded Region on Pressure Performance for the Base Case with $R_a/R_g = 6.0$.

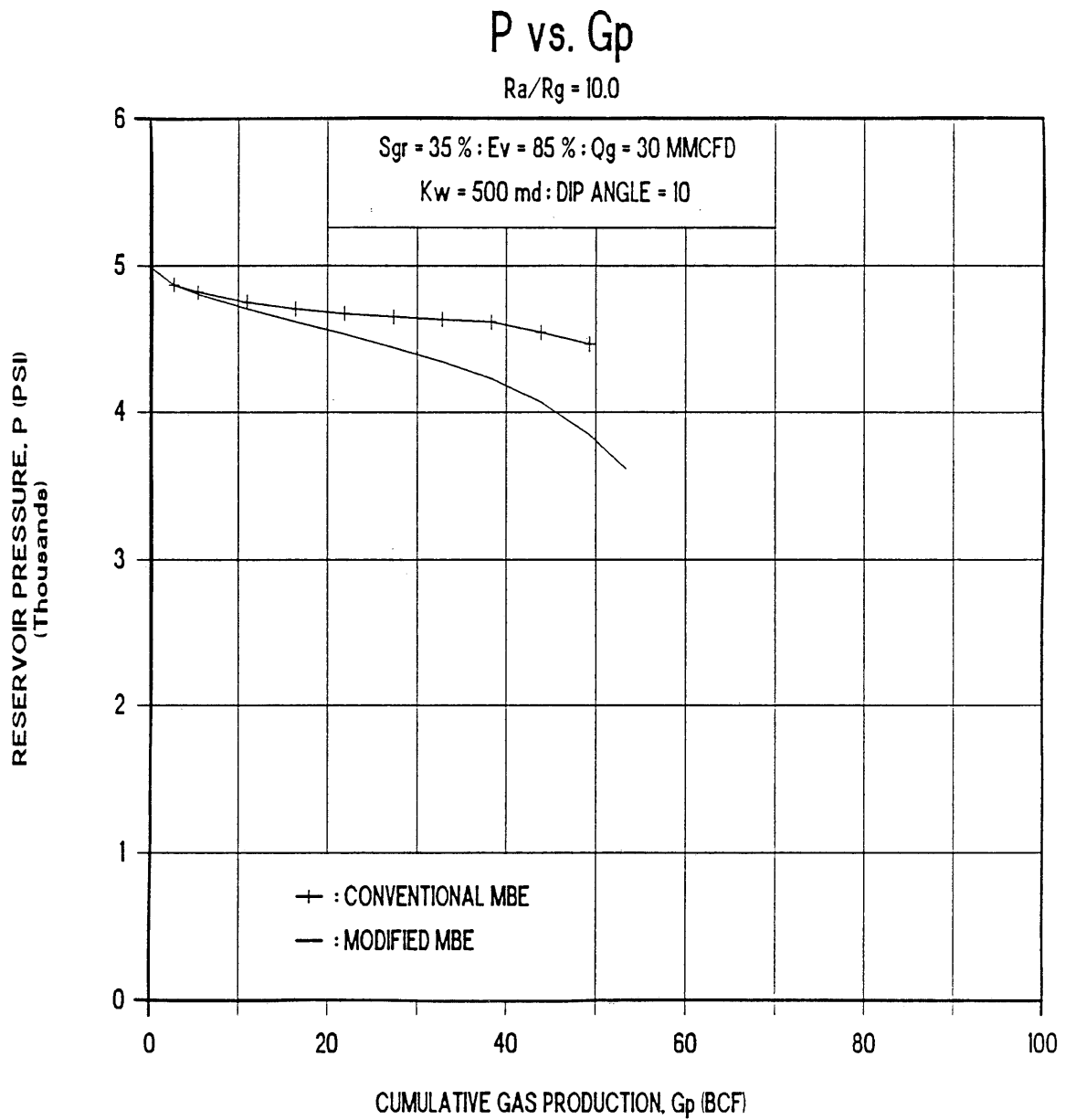


Figure 8. Effect of Pressure Gradient in the Water-Invaded Region on Pressure Performance for the Base Case with $R_a/R_g = 10.0$.

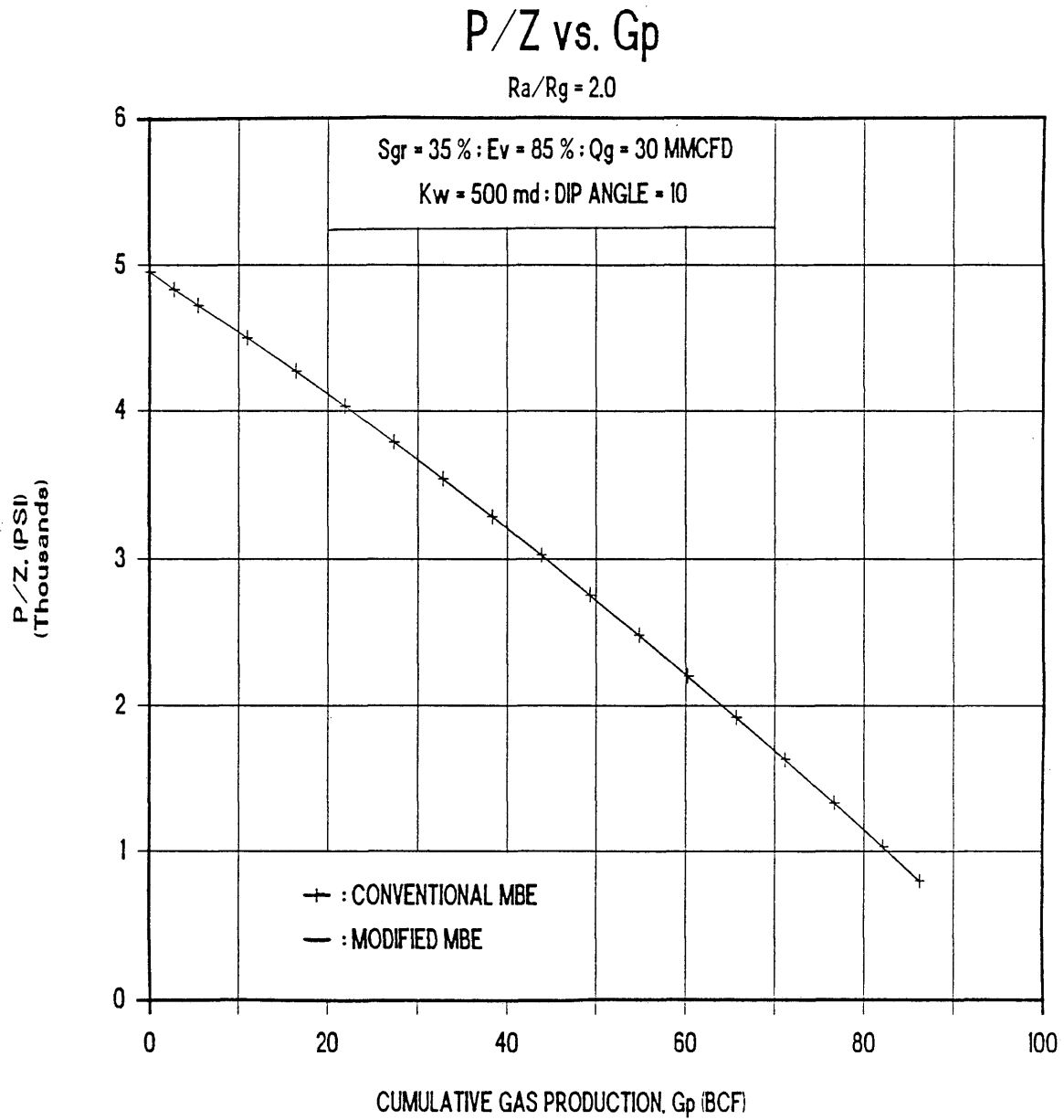


Figure 9. Effect of Pressure Gradient in the Water-Invaded Region on P/Z Performance for the Base Case with $R_a/R_g = 2.0$.

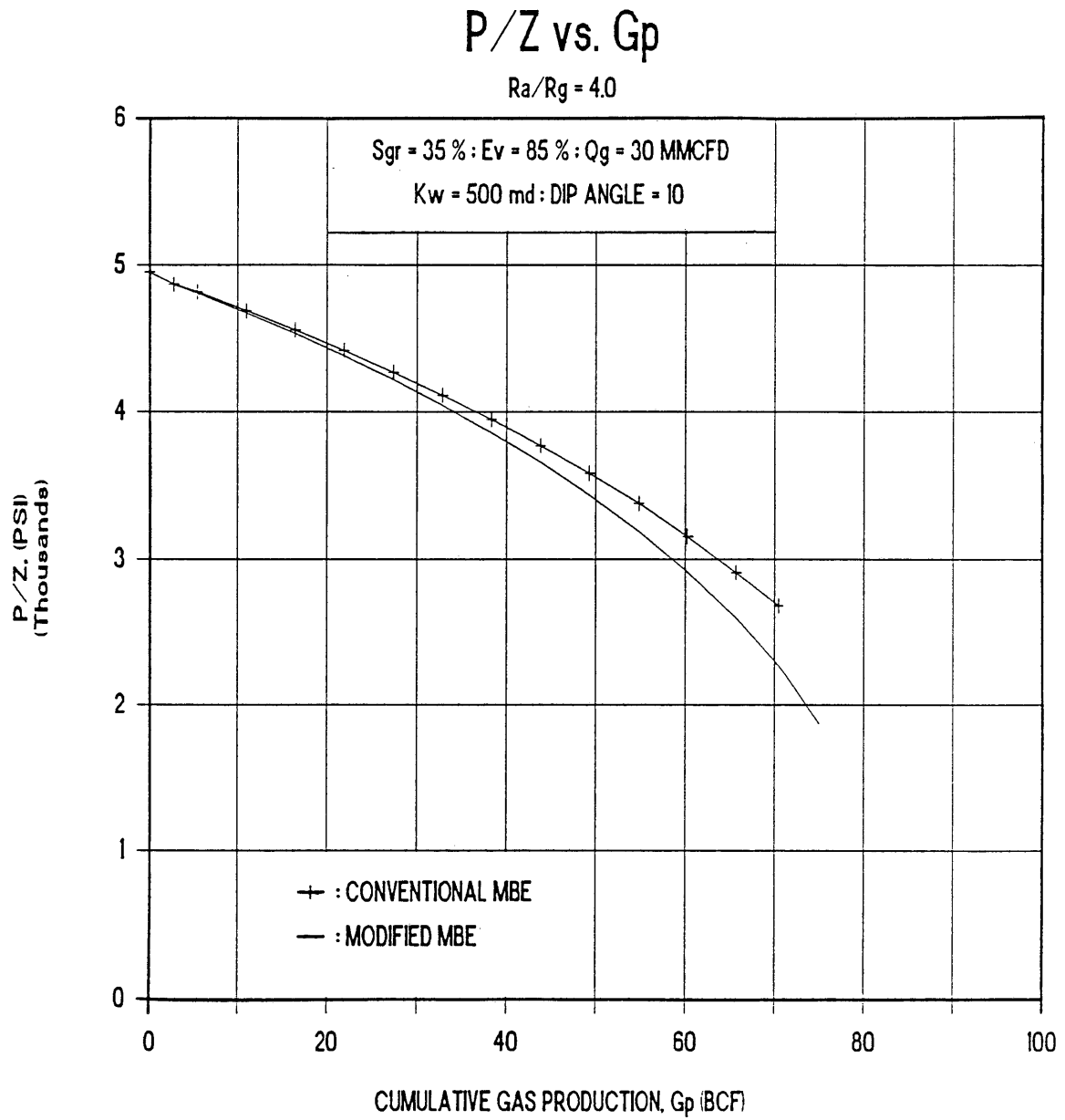


Figure 10. Effect of Pressure Gradient in the Water-Invaded Region on P/Z Performance for the Base Case with $R_a/R_g = 4.0$.

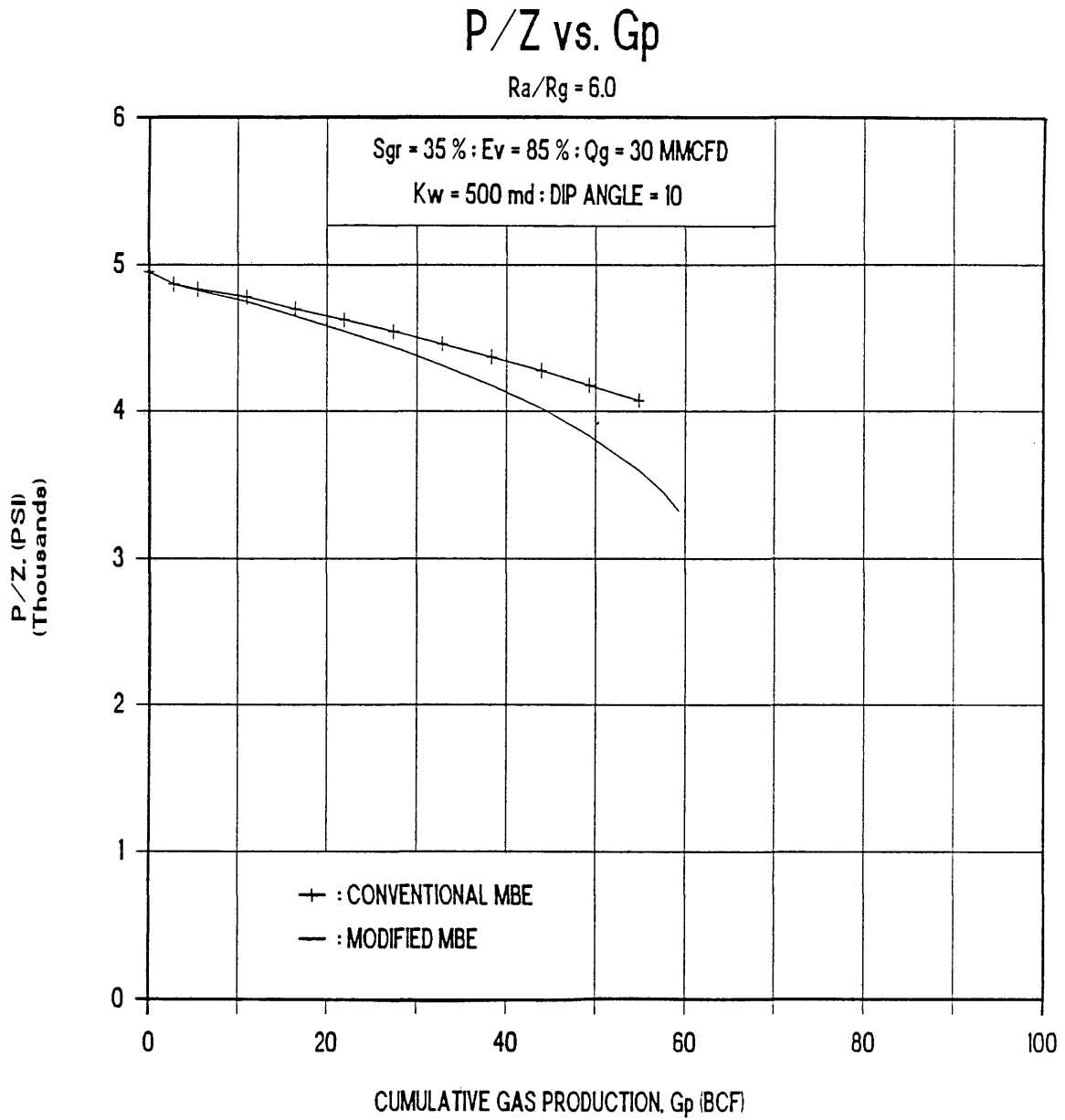


Figure 11. Effect of Pressure Gradient in the Water-Invaded Region on P/Z Performance for the Base Case with $R_a/R_g = 6.0$.

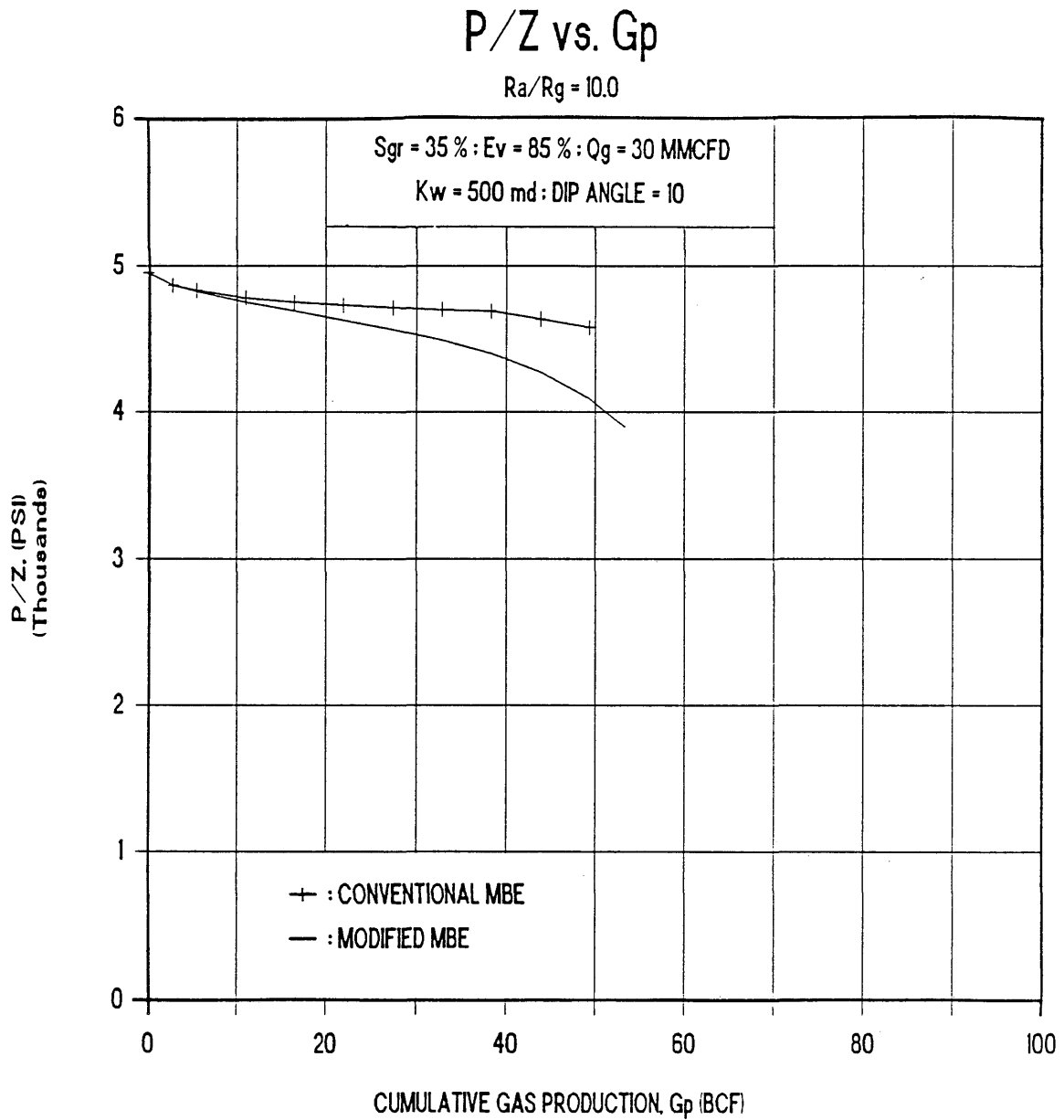


Figure 12. Effect of Pressure Gradient in the Water-Invaded Region on P/Z Performance for the Base Case with $R_a/R_g = 10.0$.

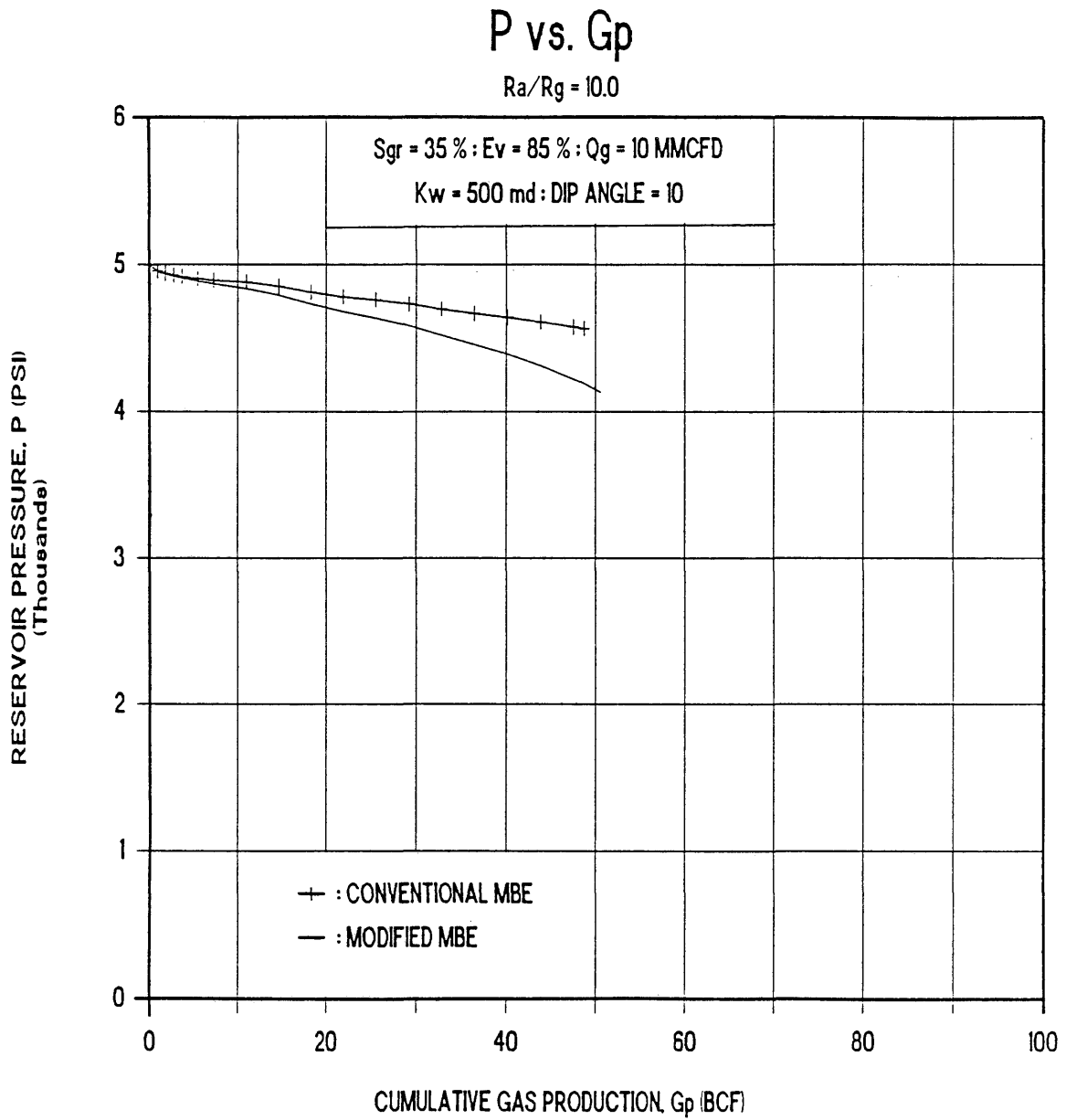


Figure 13. Effect of Pressure Gradient in the Water-Invaded Region on Pressure Performance for the Base Case with Q_g = 10 MMCFD.

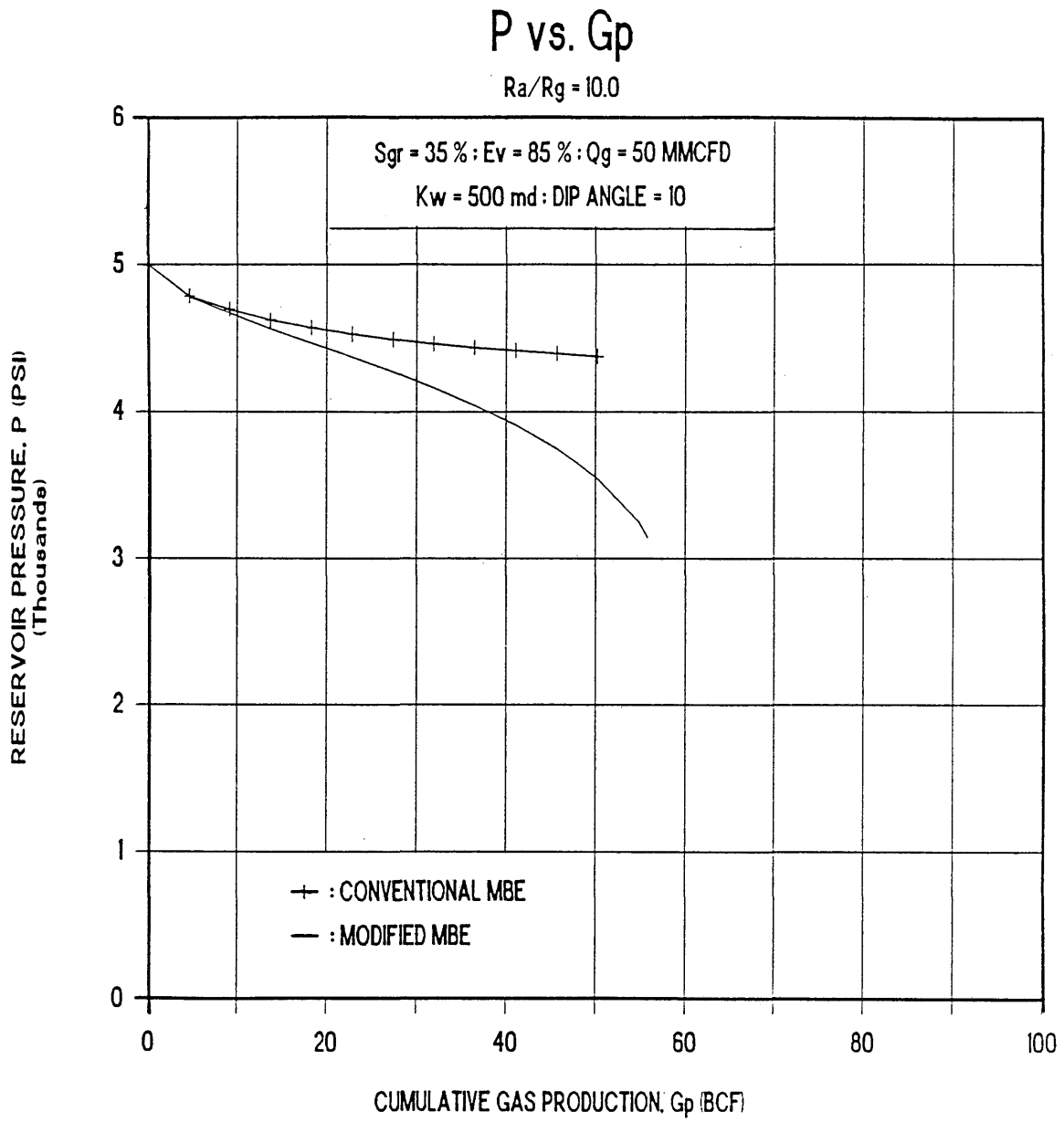


Figure 14. Effect of Pressure Gradient in the Water-Invaded Region on Pressure Performance for the Base Case with Q_g = 50 MMCFD.

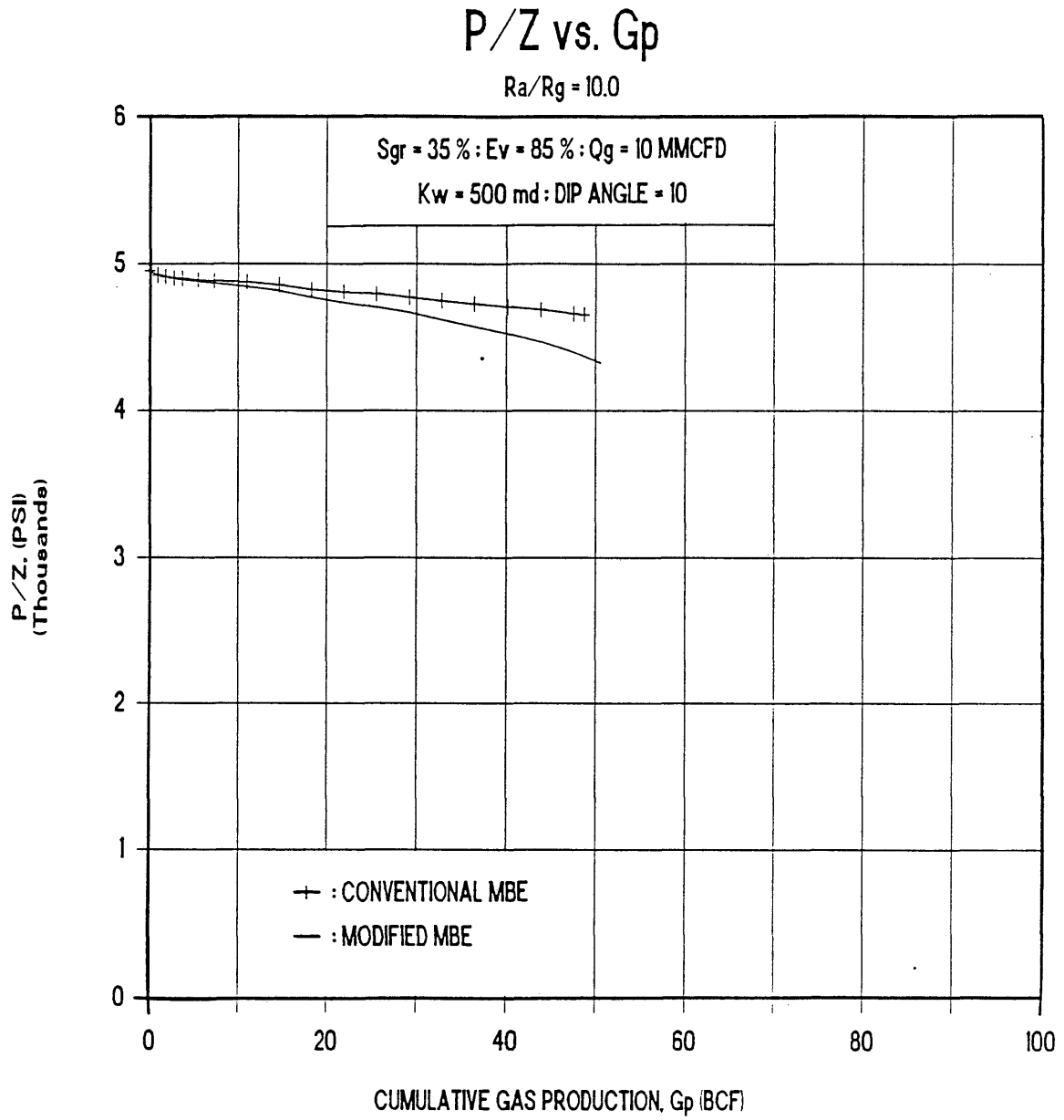


Figure 15. Effect of Pressure Gradient in the Water-Invaded Region on P/Z Performance for the Base Case with Q_g = 10 MMCFD.

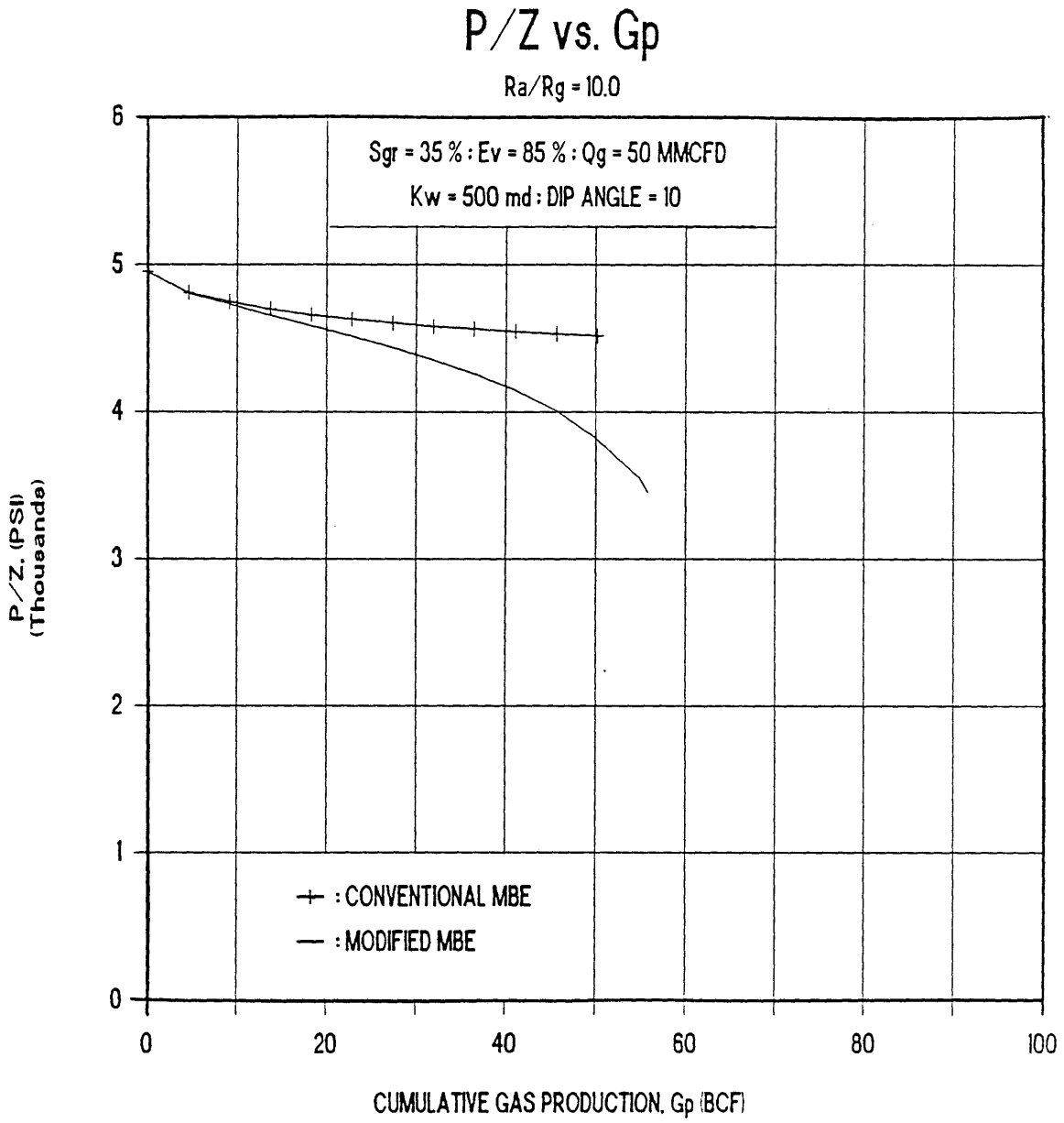


Figure 16. Effect of Pressure Gradient in the Water-Invaded Region on P/Z Performance for the Base Case with Q_g = 50 MMCFD.

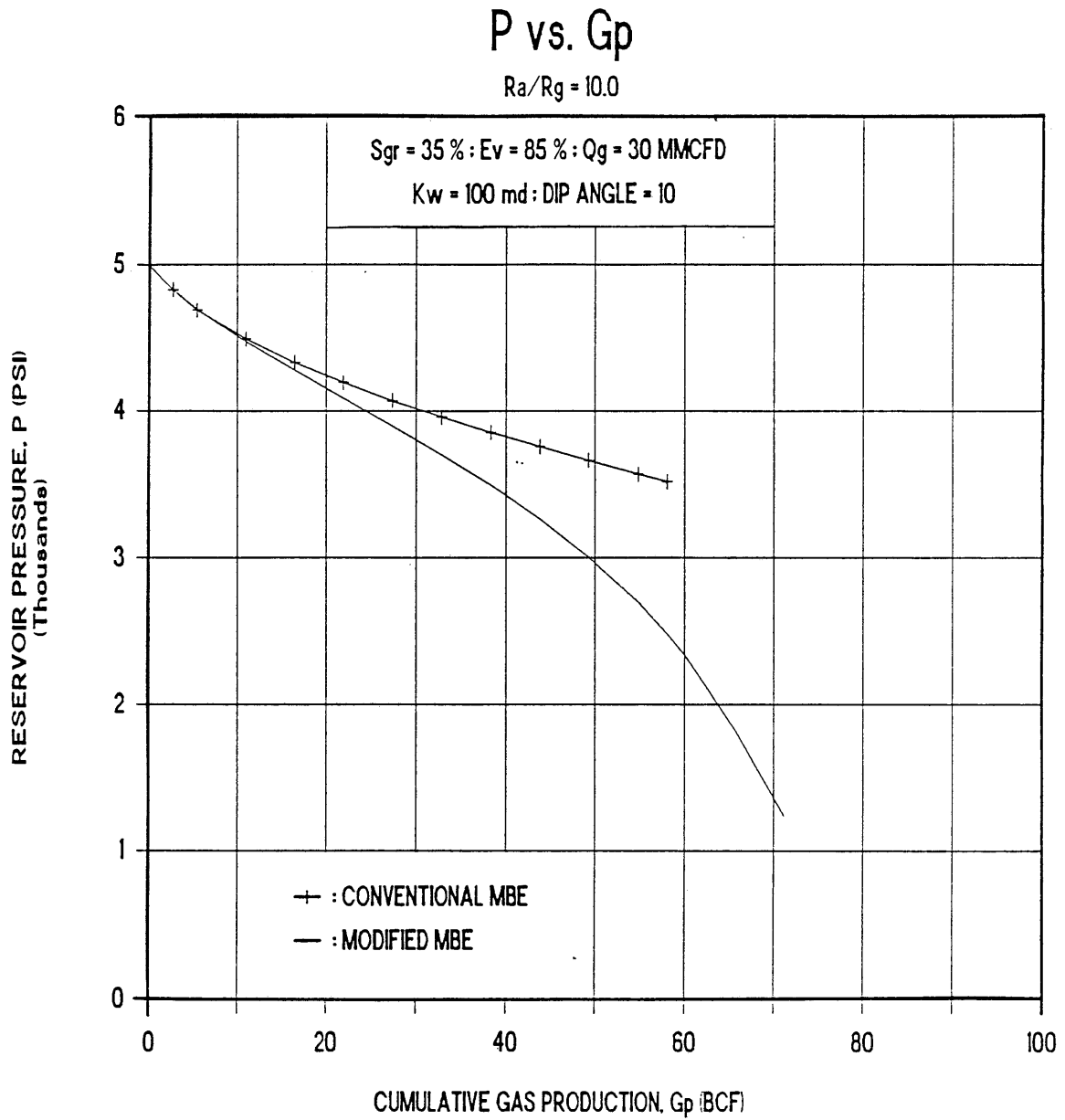


Figure 17. Effect of Pressure Gradient in the Water-Invaded Region on Pressure Performance for the Base Case with $K_w = 100$ md.

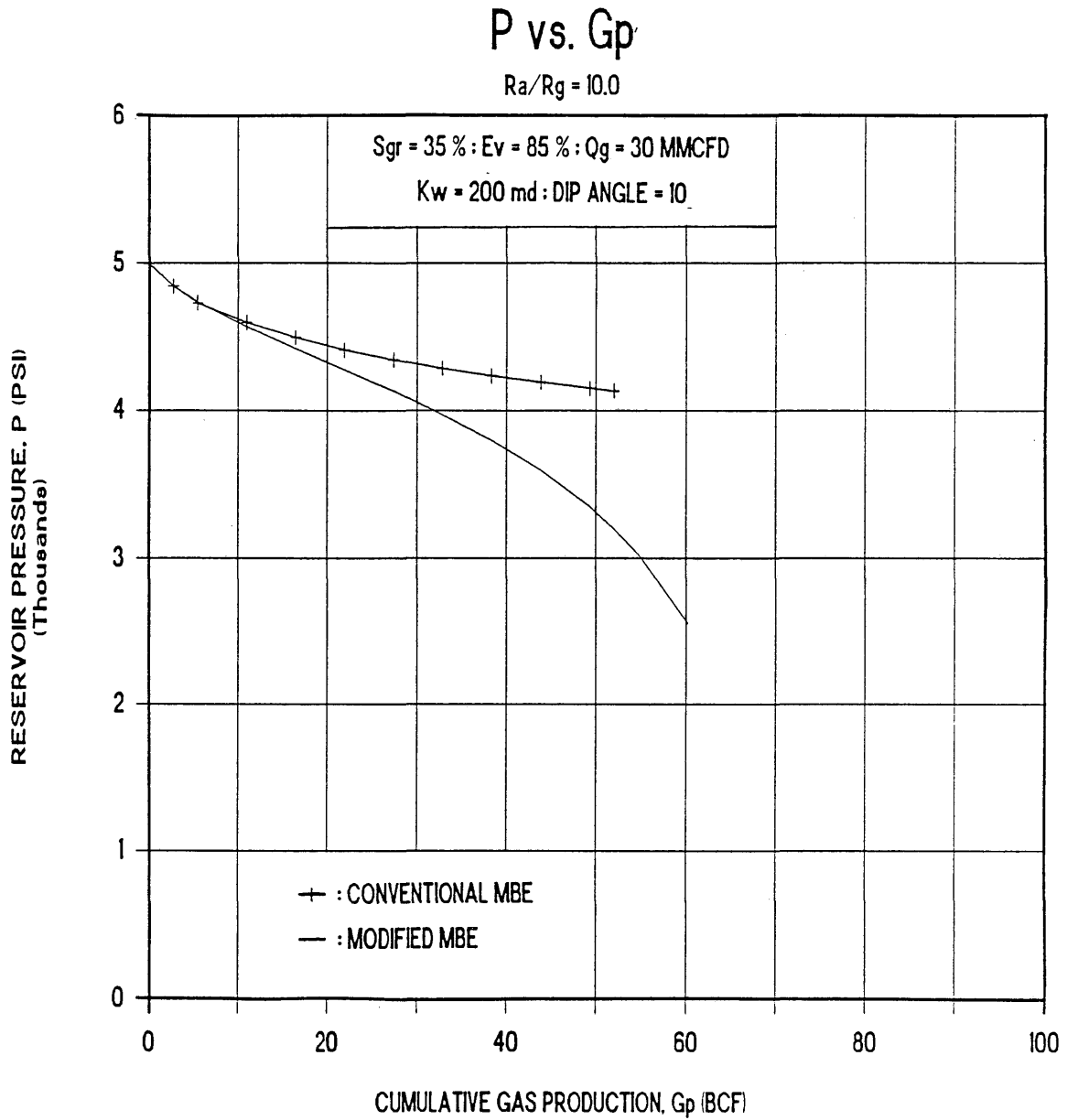


Figure 18. Effect of Pressure Gradient in the Water-Invaded Region on Pressure Performance for the Base Case with $K_w = 200$ md.

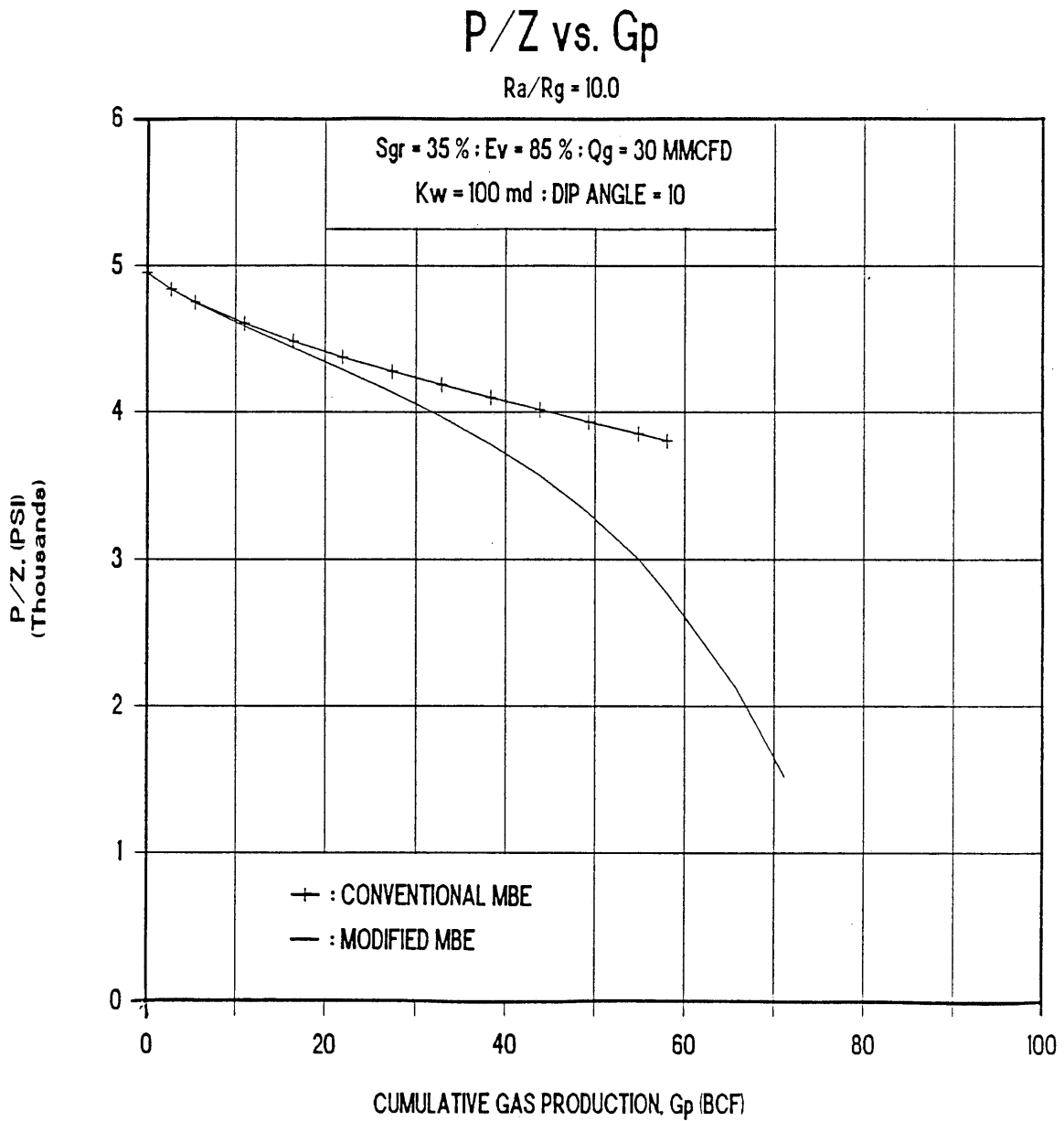


Figure 19. Effect of Pressure Gradient in the Water-Invaded Region on P/Z Performance for the Base Case with $K_w = 100$ md.

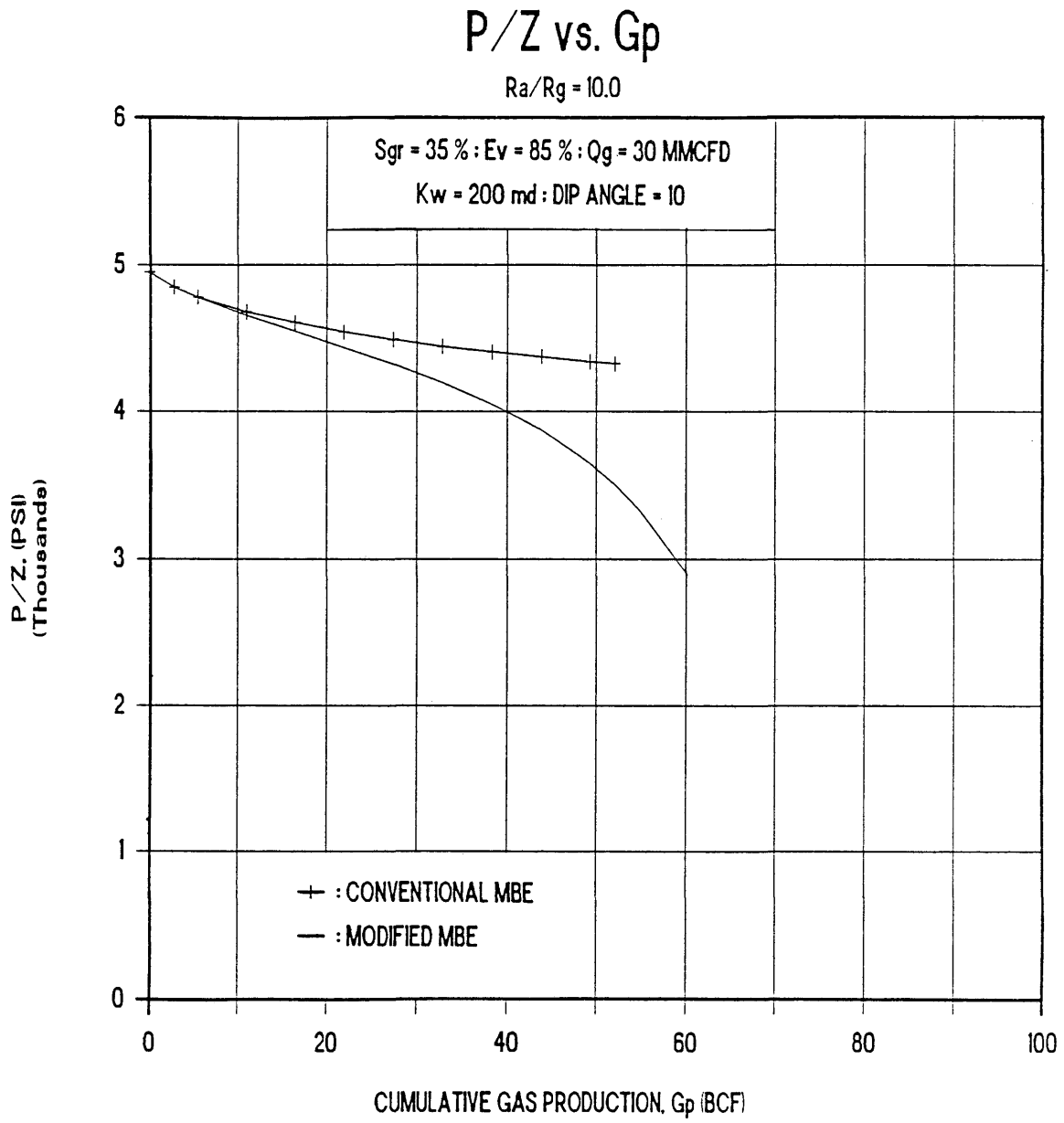


Figure 20. Effect of Pressure Gradient in the Water-Invaded Region on P/Z Performance for the Base Case with K_w = 200 md.

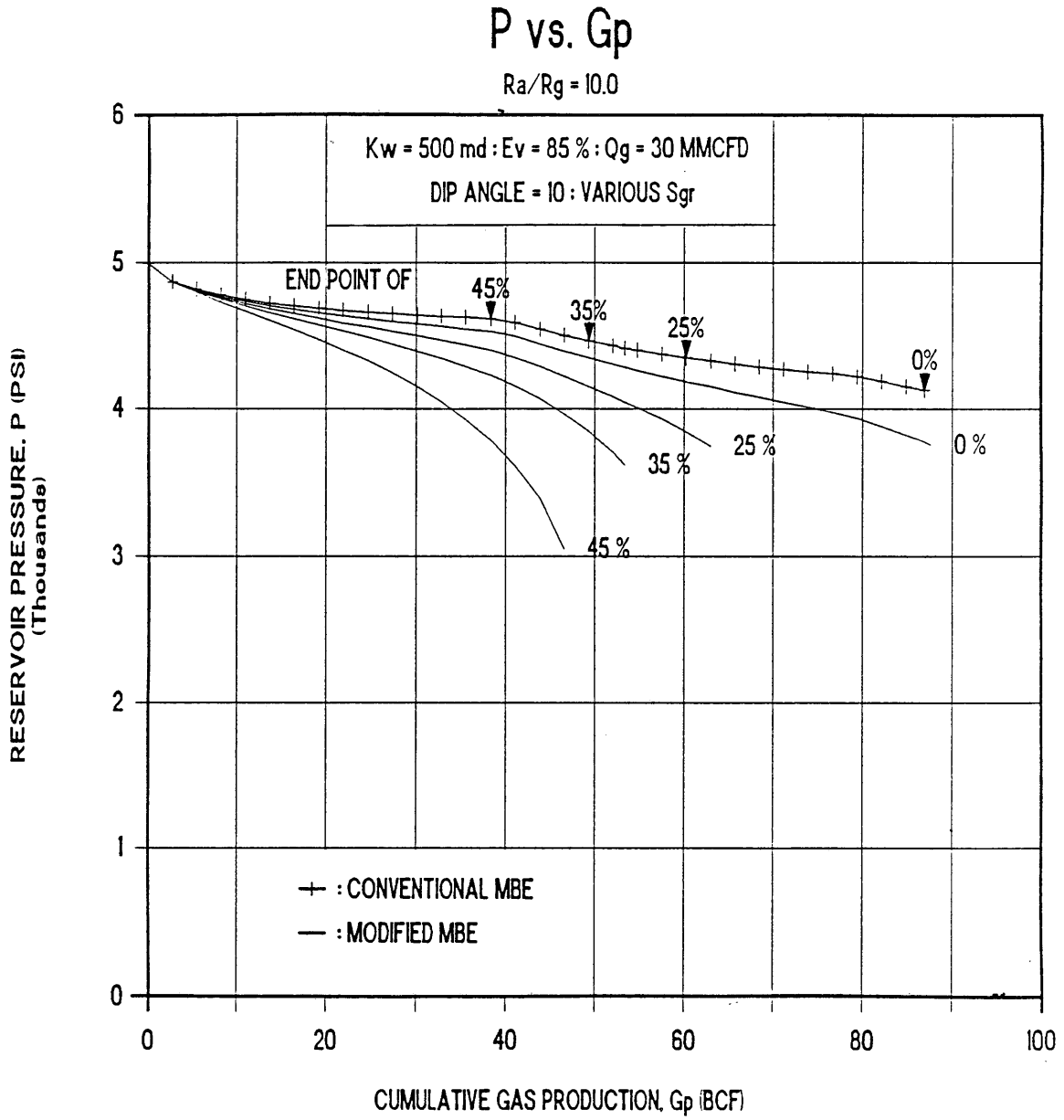


Figure 21. Effect of Pressure Gradient in the Water-Invaded Region on Pressure Performance for the Base Case with various Values of S_{gr}.

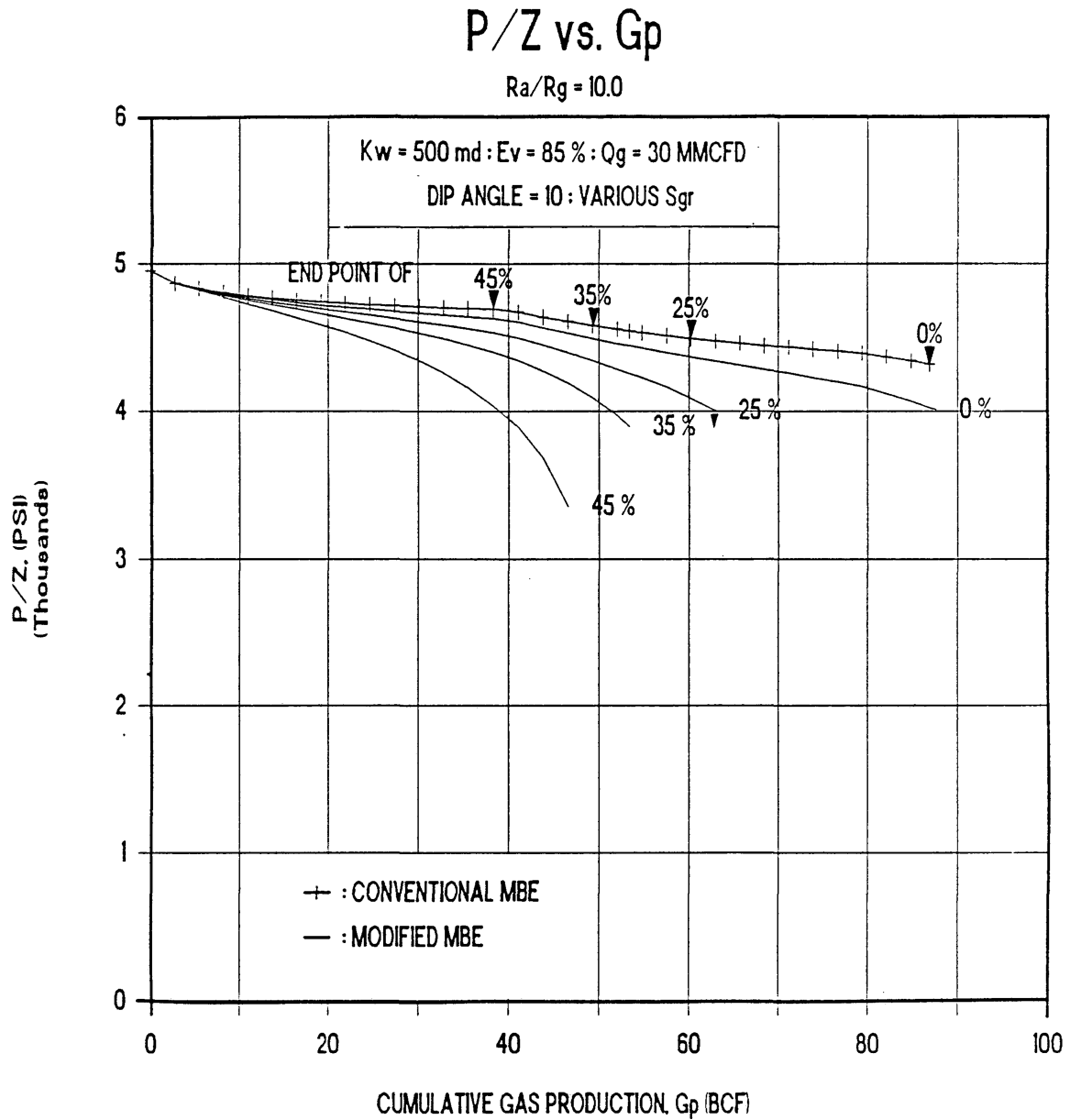


Figure 22. Effect of Pressure Gradient in the Water-Invaded Region on P/Z Performance for the Base Case with various Values of S_{gr} .

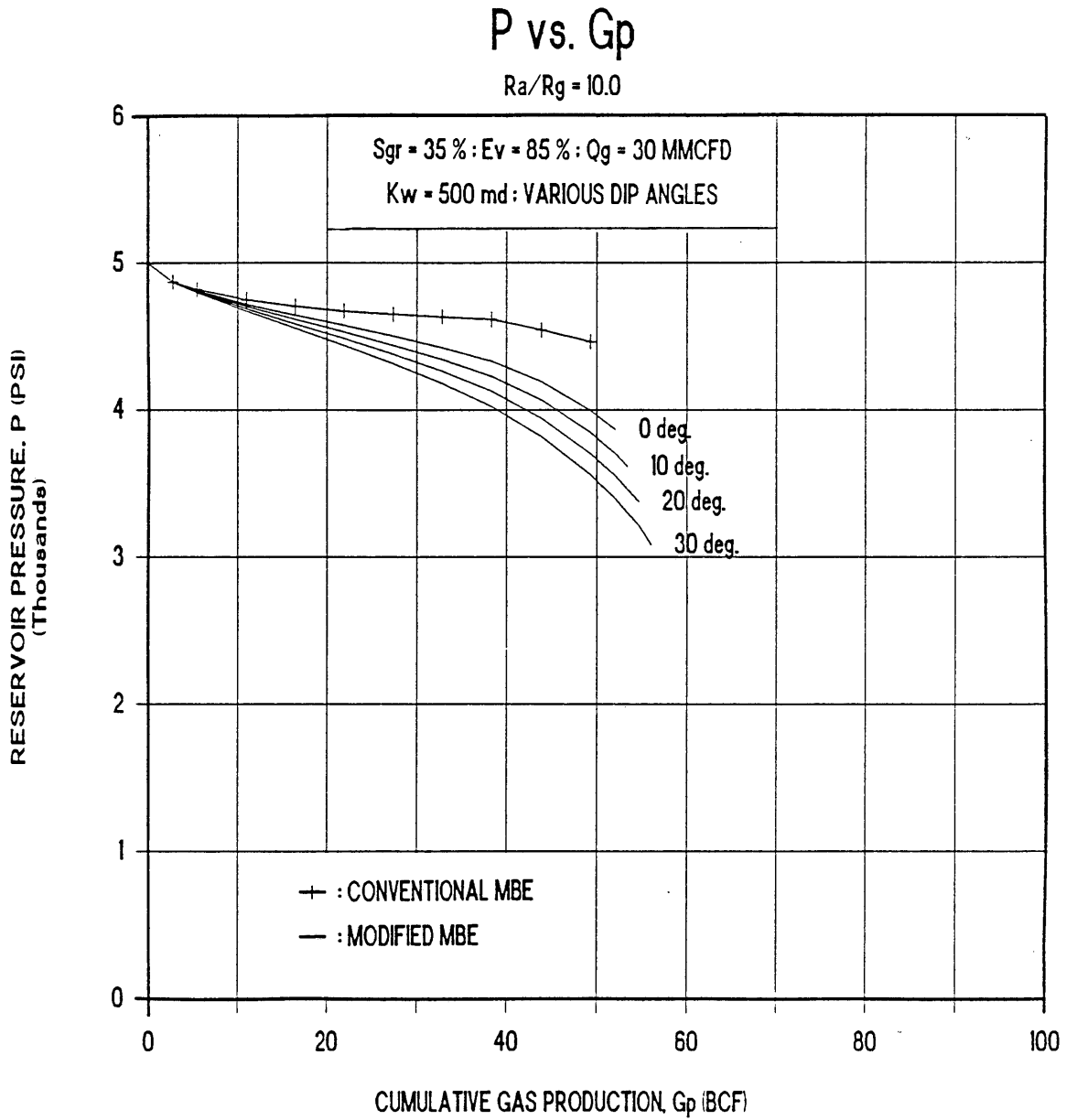


Figure 23. Effect of Pressure Gradient in the Water-Invaded Region on Pressure Performance for the Base Case with various Dip Angles.

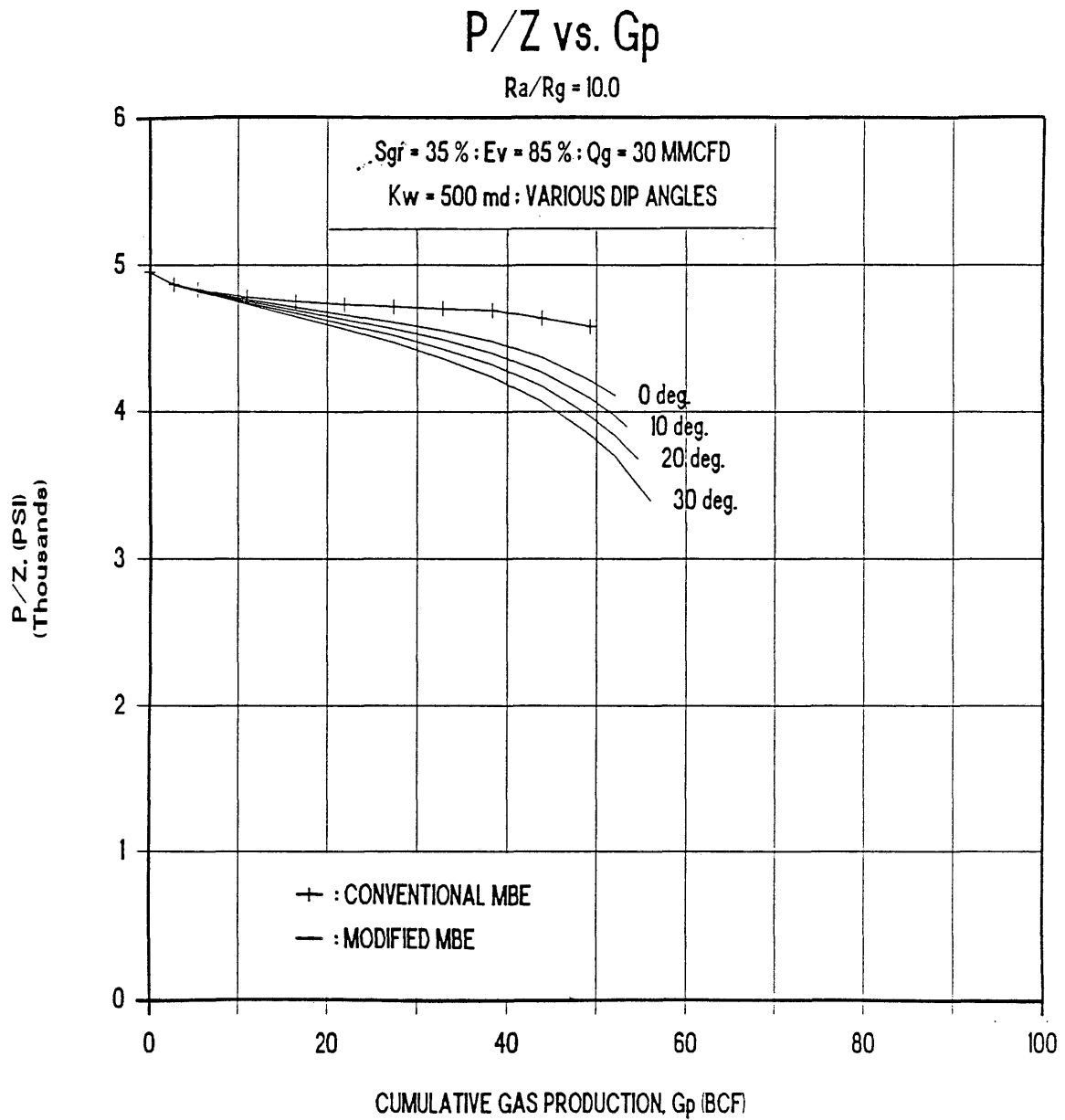


Figure 24. Effect of Pressure Gradient in the Water-Invaded Region on P/Z Performance for the Base Case with various Dip Angles.

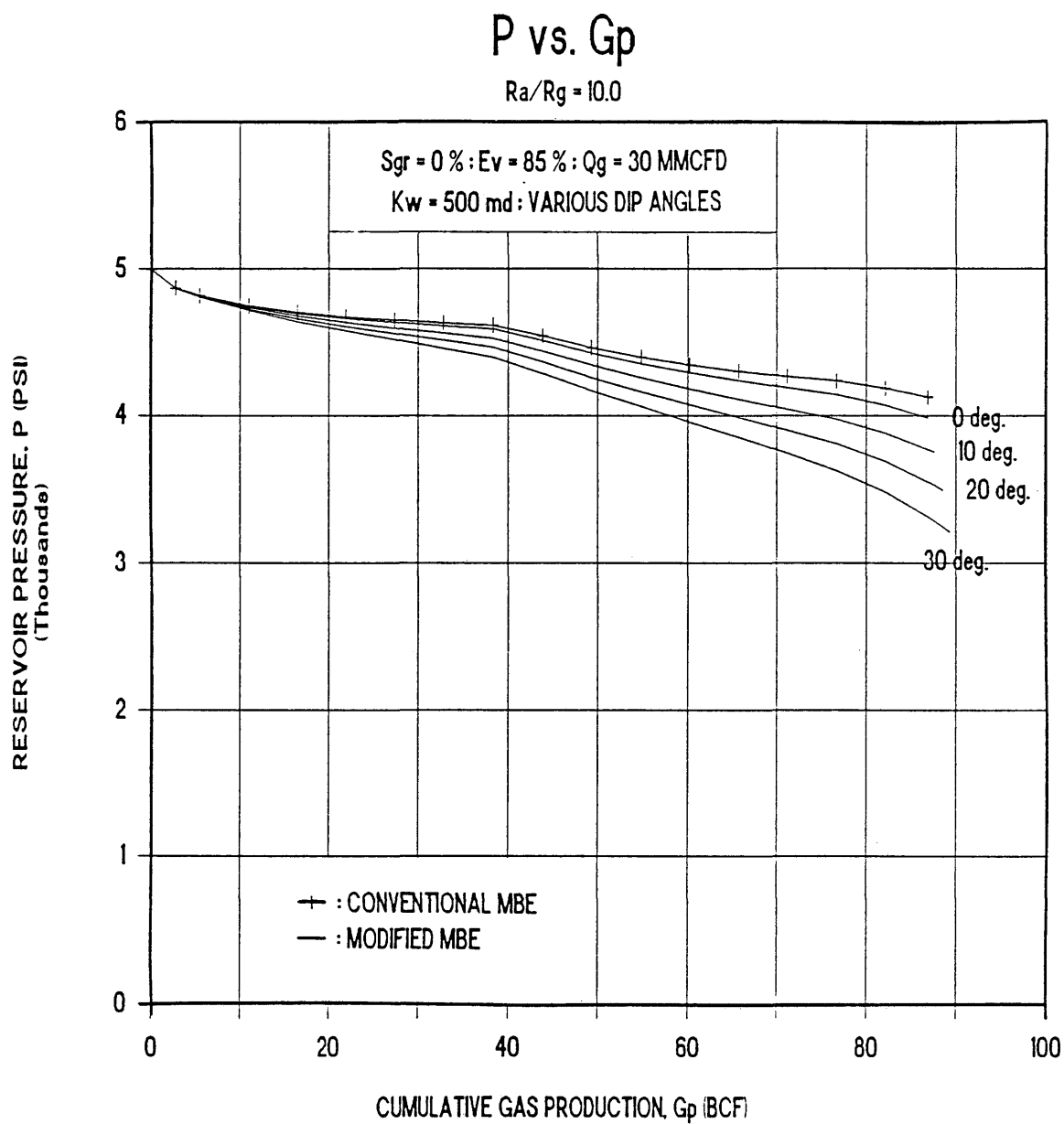


Figure 25. Effect of Pressure Gradient in the Water-Invaded Region on Pressure Performance for the Base Case with $S_{gr} = 0\%$, and various Dip Angles.

PRESSURE ERROR vs. Gp

VARIOUS R_a/R_g

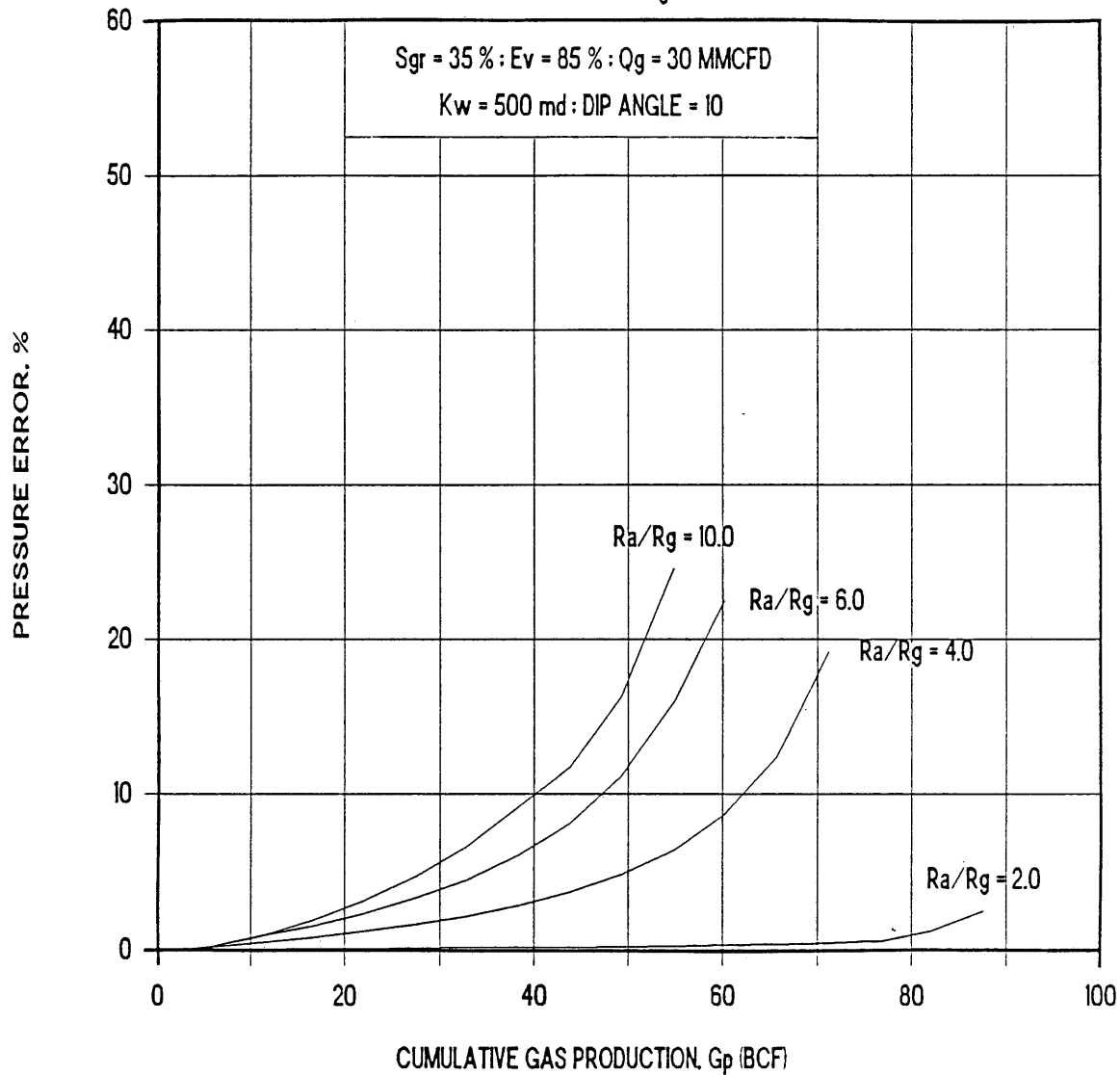


Figure 26. Percent Error in Pressure Prediction Caused by Omission of Pressure Gradient in the Water-Invaded Region for the Base Case with various Values of R_a/R_g .

PRESSURE ERROR vs. G_p

$R_a/R_g = 10.0$

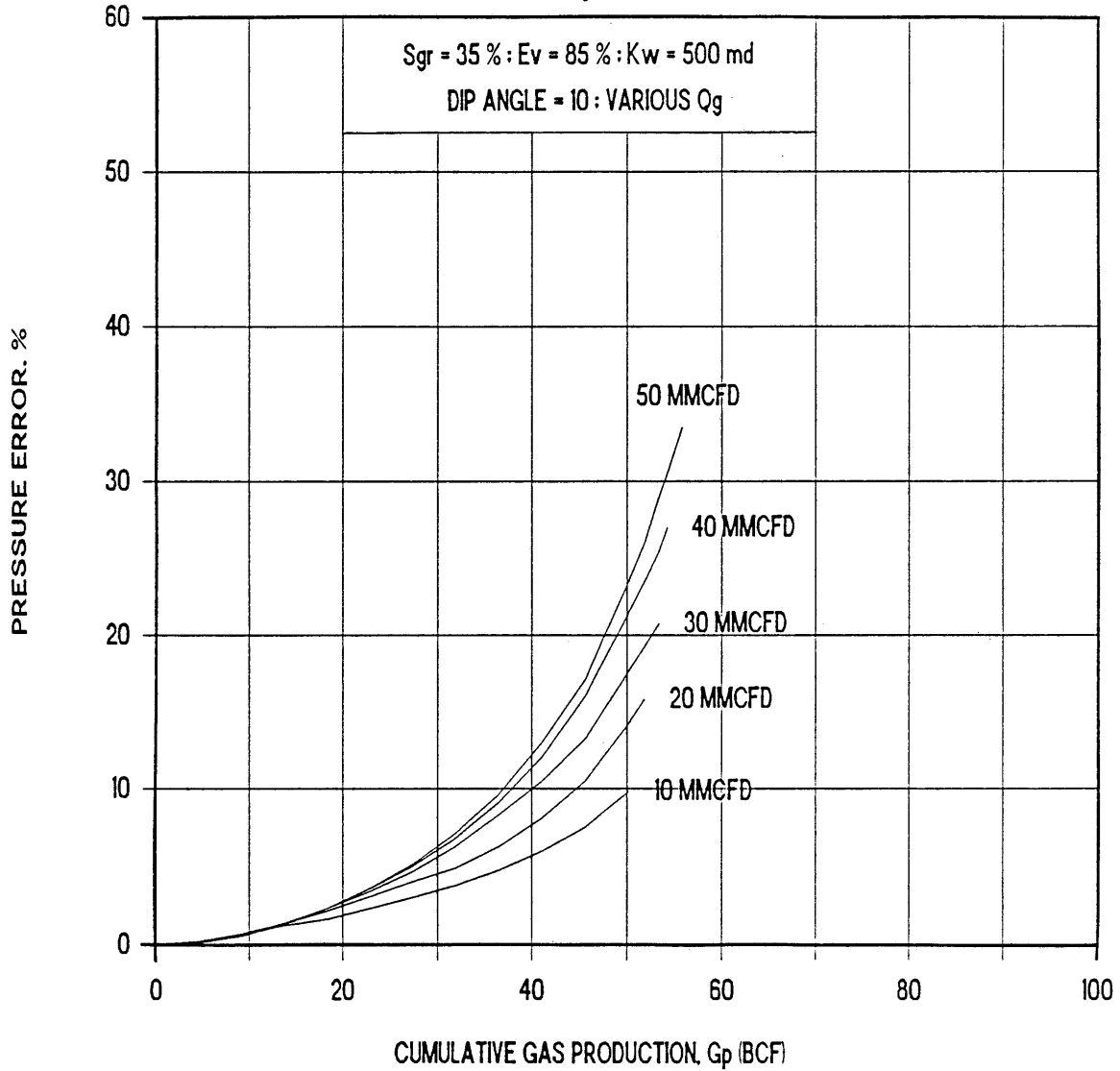


Figure 27. Percent Error in Pressure Prediction Caused by Omission of Pressure Gradient in the Water-Invaded Region for the Base Case with various Values of Q_g .

PRESSURE ERROR vs. Gp

$R_a/R_g = 10.0$

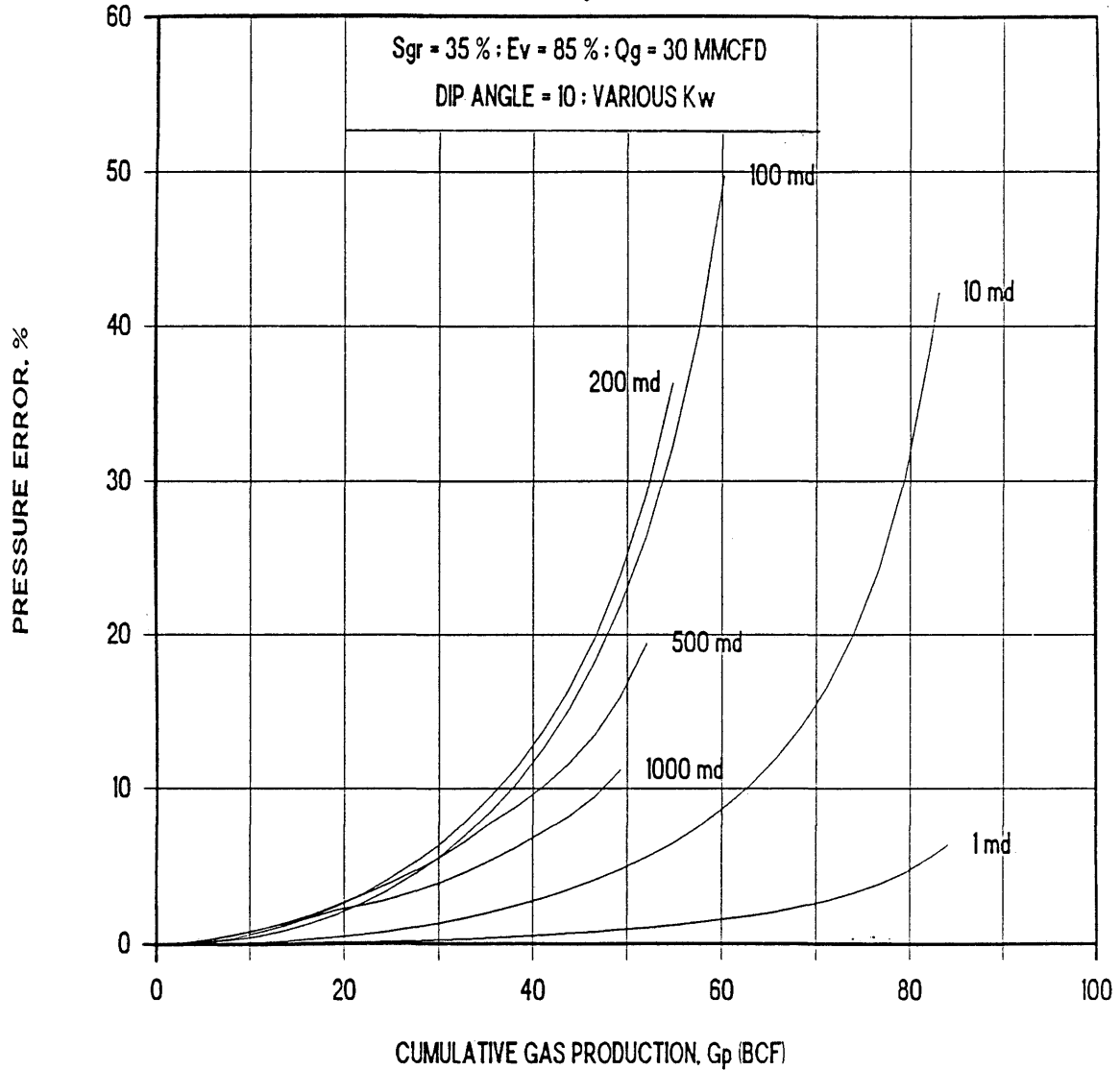


Figure 28. Percent Error in Pressure Prediction Caused by Omission of Pressure Gradient in the Water-Invaded Region for the Base Case with various Values of K_w .

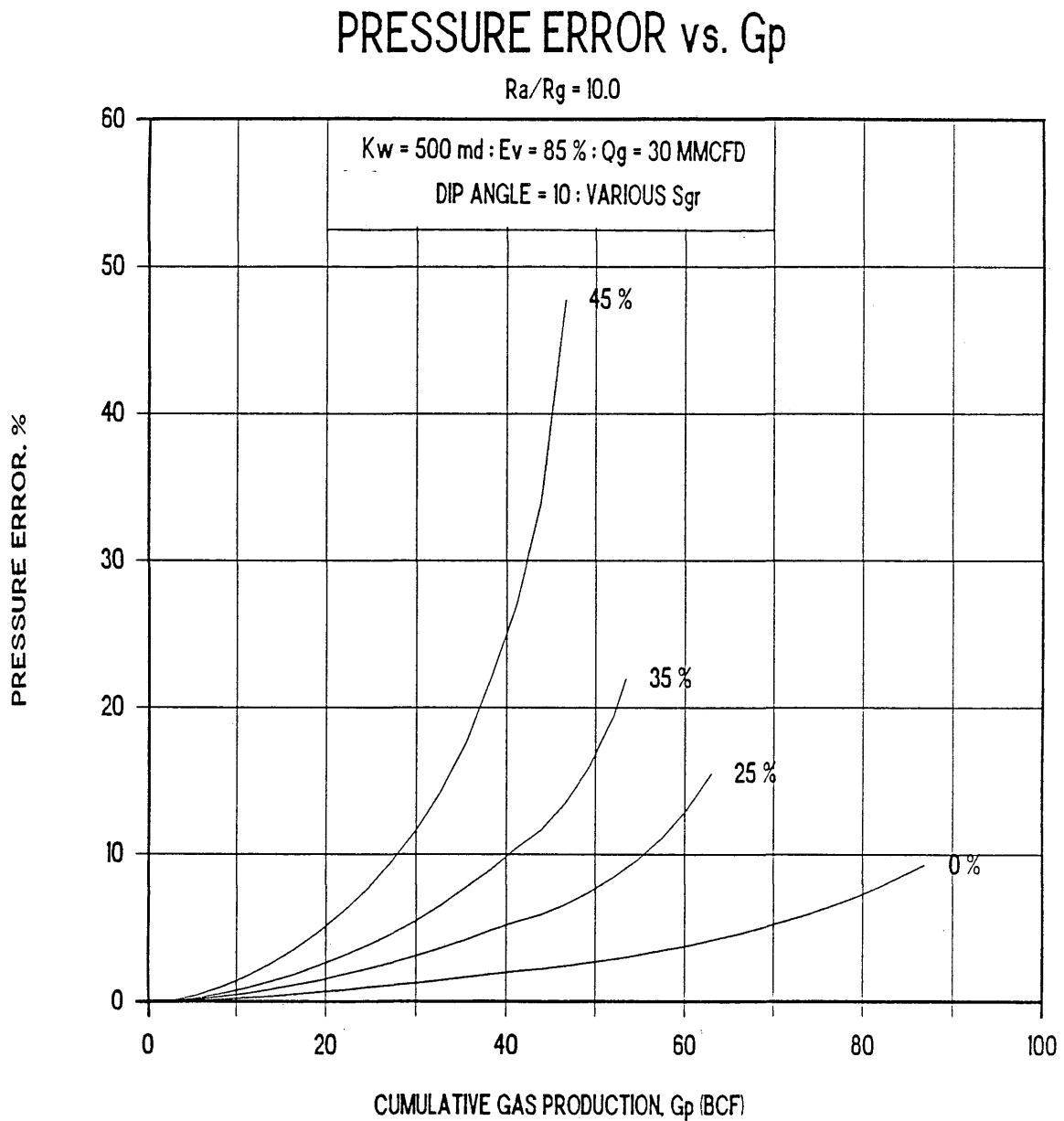


Figure 29. Percent Error in Pressure Prediction Caused by Omission of Pressure Gradient in the Water-Invaded Region for the Base Case with various Values of S_{gr} .

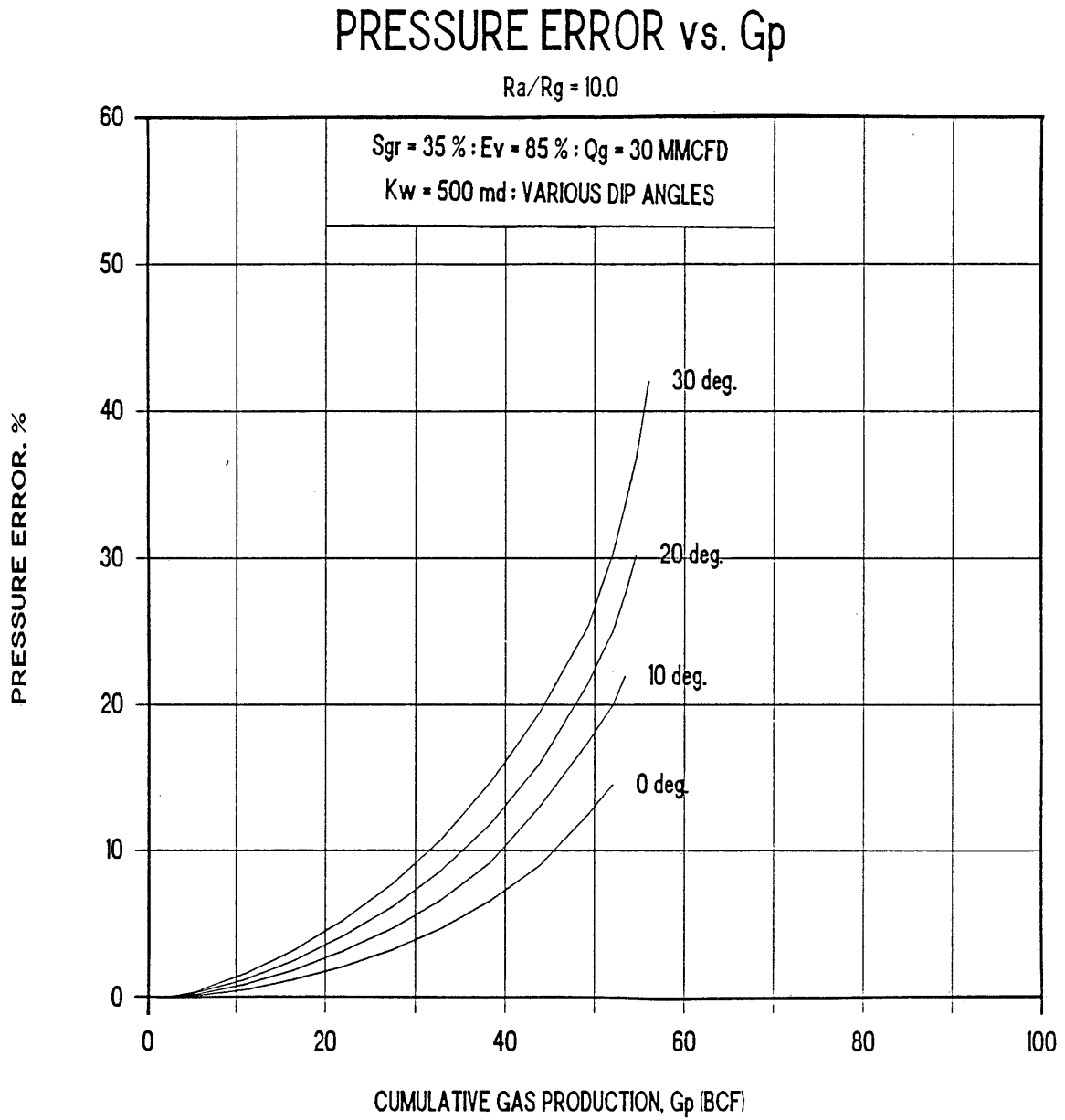


Figure 30. Percent Error in Pressure Prediction Caused by Omission of Pressure Gradient in the Water-Invaded Region for the Base Case with various Dip Angles.

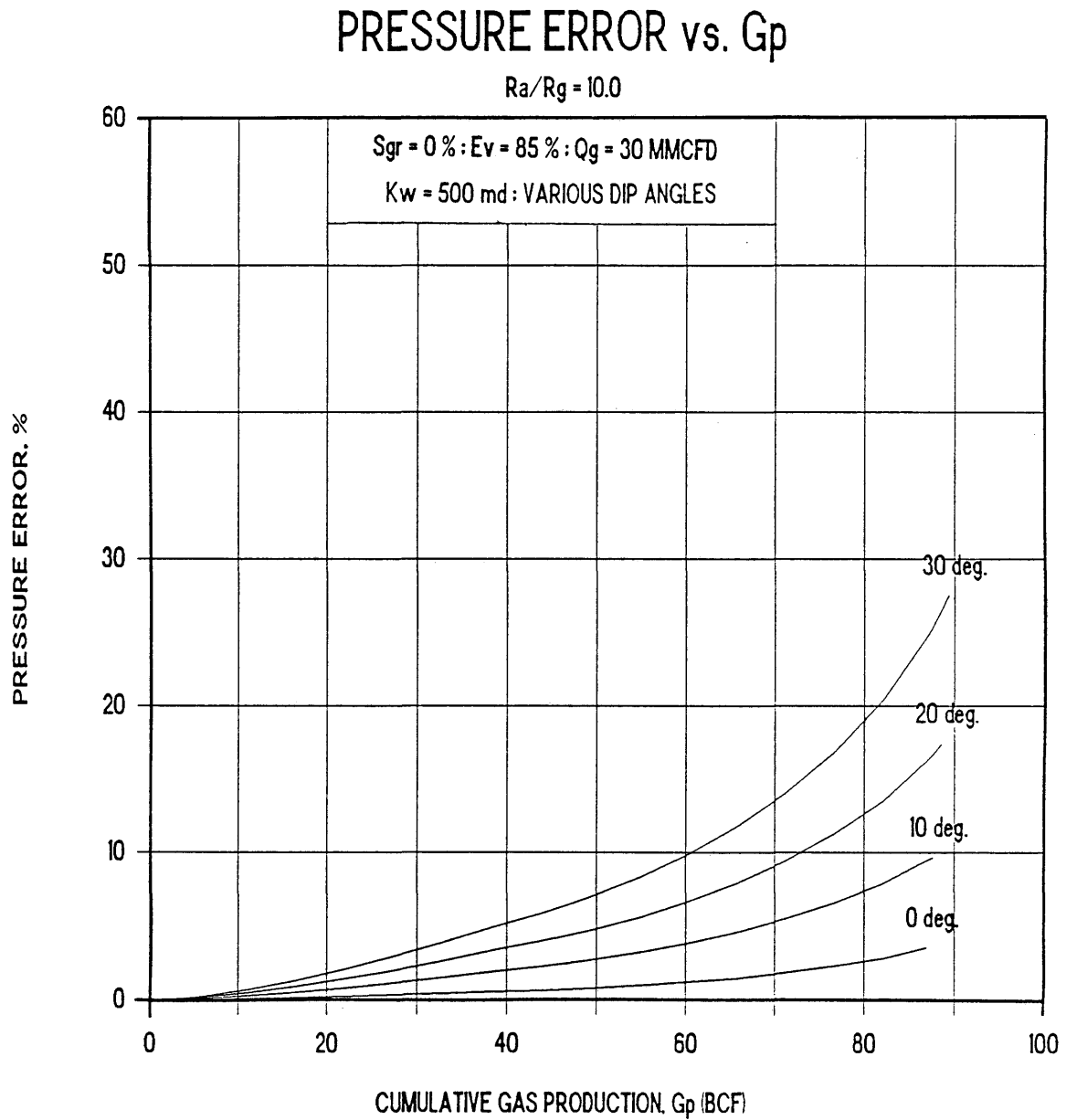


Figure 31. Percent Error in Pressure Prediction Caused by Omission of Pressure Gradient in the Water-Invaded Region for the Base Case with $S_{gr} = 0\%$, and various Dip Angles.

PRESSURE ERROR vs. G_p

R_a/R_g = 10.0

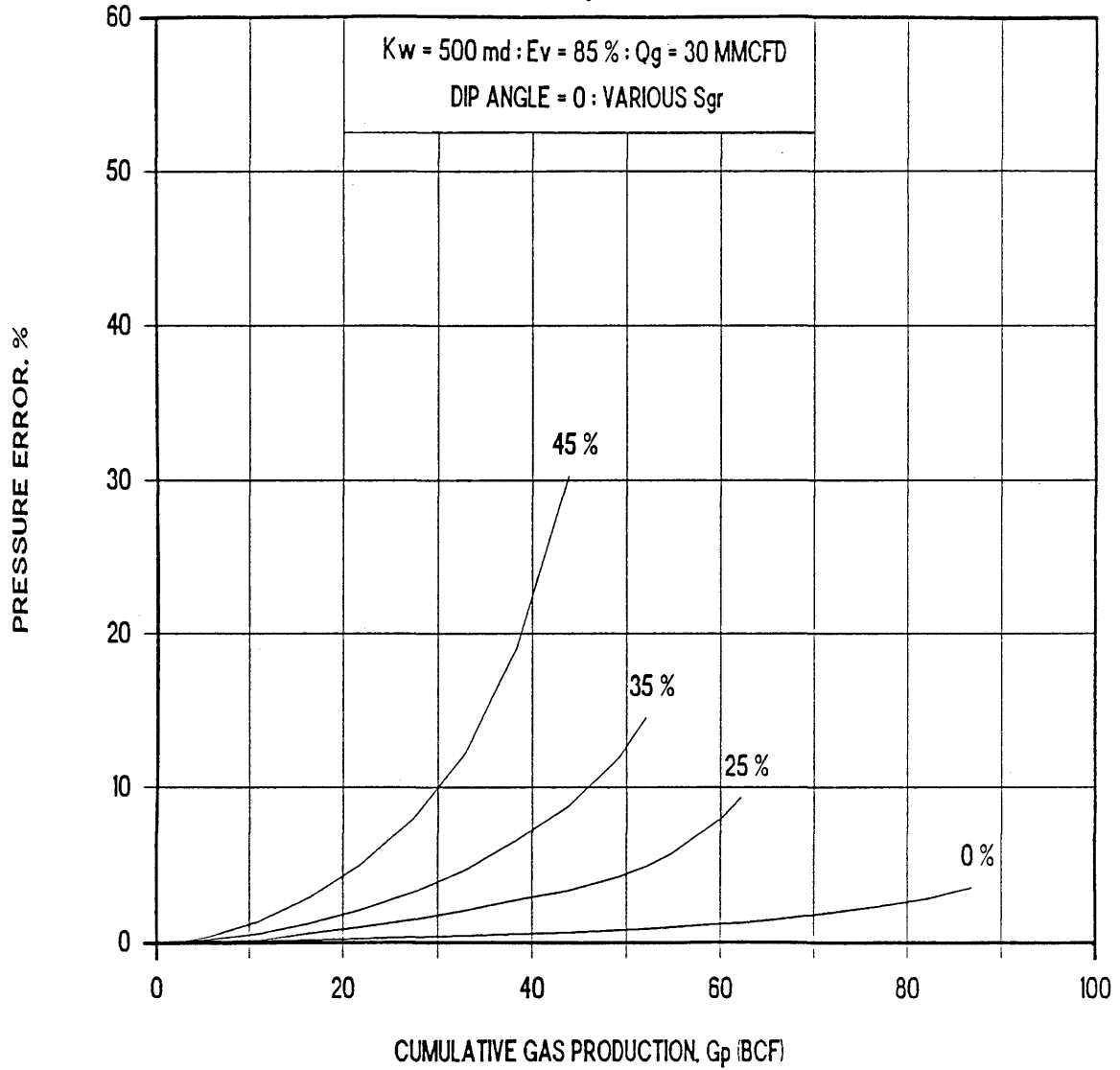


Figure 32. Percent Error in Pressure Prediction Caused by Omission of Pressure Gradient in the Water-Invaded Region for the Base Case with Dip Angles = 0, and various Values of S_{gr}.

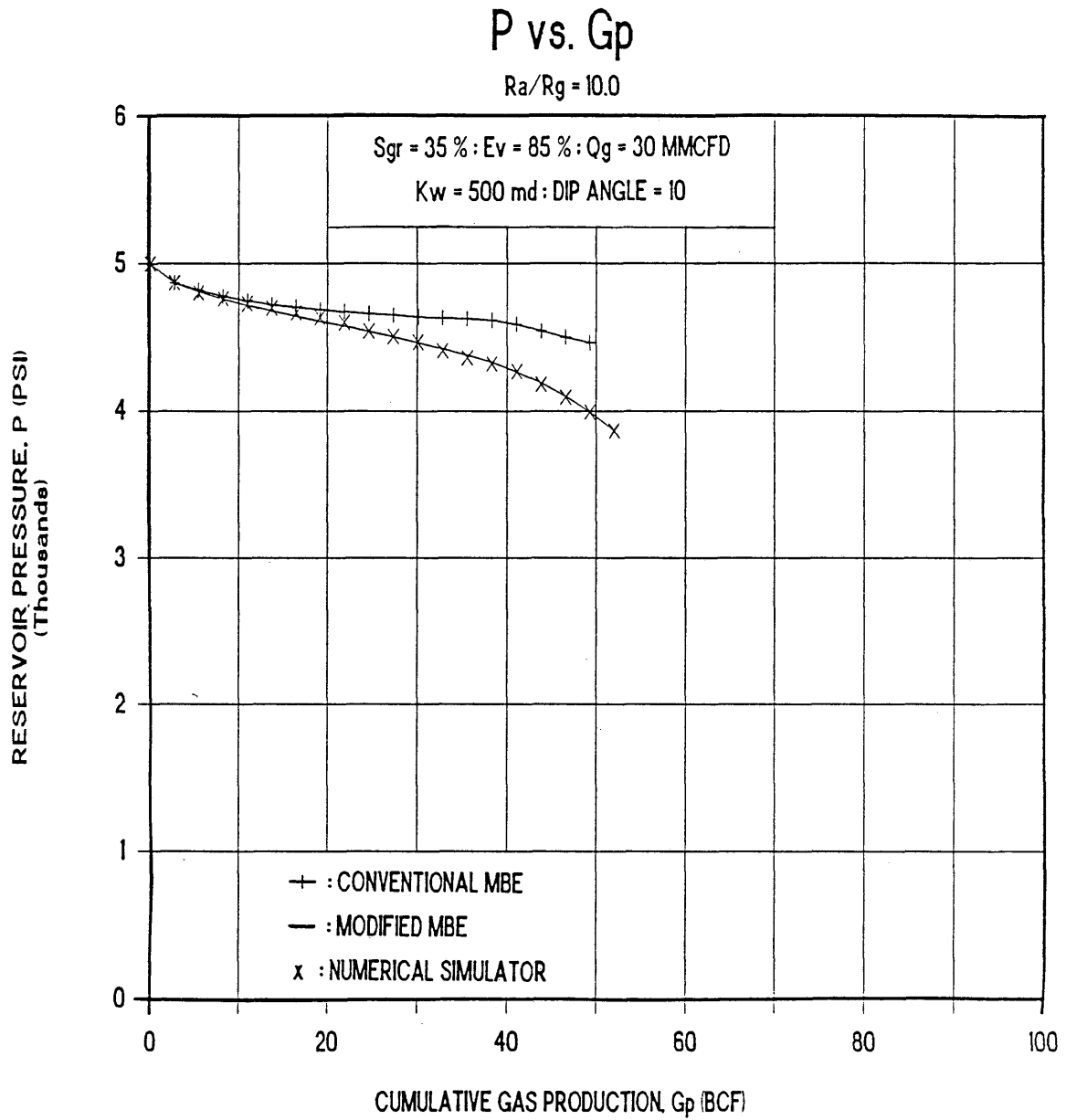


Figure 33. Comparison of Pressure Performance Predictions using Three Different Methods: Conventional MBE, Modified MBE, and Numerical Simulator.

APPENDIX A

SAMPLE CALCULATIONS

Given data:

OGIP	= 100 BCF
initial pressure	= 5000 psia
thickness	= 30 ft
reservoir temperature	= 675 °R
volumetric sweep eff.	= 85 %
porosity	= .25
gas spec. gravity	= .65
water viscosity	= .7 cp
water spec. gravity	= 1.02
initial water saturation	= .25
water compressibility	= 4XE-6
rock compressibility	= 5XE-6
aquifer permeability	= 500 md
residual gas saturation	= 35 %
R_a/R_g	= 10
gas rate	= 30 MMCFD
dip angle	= 10 degree
time step	= 91.25 days

Conventional Material Balance Method

1. Calculate gas reservoir radius using eq. 8.

$$R_g = \left[\frac{(5.6146)(100E9)(.000686)}{(3.1416)(30)(.25)(1)(.75)} \right]^{0.5} = 4668.27 \text{ ft.}$$

2. Calculate G_p . for a fixed time increment of 91.25 days.

$$G_p = 91.25 * 30E6 = 2.7375 \text{ BCF}$$

3. Estimate reservoir pressure, $P = 4820$ psia, and calculate

$$P/Z = 4833 \text{ psia, and}$$

$$B_g = 0.000703 \text{ rb/scf}$$

4. Solve eq. 4 for W_{em} (material balance).

$$\begin{aligned} W_{em} &= (2.7375E9 * .000703) - 100E9*(.000703 - .000686) \\ &= 200,114 \text{ bbl.} \end{aligned}$$

5. Solve eq. 5 for W_e aquifer.

$$\begin{aligned} B &= (1.1191) (.25) (9E-6) (30) (4668.27)^2 (1) \\ &= 1646.21 \text{ bbl/psia.} \end{aligned}$$

$$\Delta P = (5000 - 4820)/2 = 90 \text{ psia}$$

$$t_D = \frac{(.006323) (500) (91.25)}{(.25) (.7) (9E-6) (4668.27)^2} = 8.405$$

From the $R_a/R_g = 10$ curve of dimensionless influx unit, W_{eD} , find corresponding to $t_D = 8.405$.

$$W_{eD} = 6.539$$

$$\begin{aligned} W_e \text{ aq.} &= 1646.21 * 90 * 6.539 \\ &= 968,811 \text{ bbl.} \end{aligned}$$

6. Compare W_e calculated from step 4 with that calculated

from step 5.

$$W_{em} - W_e \text{ aq.} = |200,114 - 969,811| = 768,697 \text{ bbl.}$$

Since $|W_{em} - W_e \text{ aq.}| > 1000$ (tolerance), go to step 3, assume new pressure, and repeat the procedure until the difference between $|W_{em} - W_e \text{ aq.}|$ less than tolerance.

After iterating several times the final pressure and P/Z were 4870.24 psia and 4868.77 psia, respectively.

7. Solve eq. 19 for P/Z at abandonment condition.

$$P_a/Z_a = 9063.16 \text{ psia}$$

8. Repeat steps 2 through 7 for next time step until G_p equals G or P_a/Z_a less than P/Z step 3.

Modified Material Balance Method

1. Calculate gas reservoir radius using eq. 8.

$$R_g = \left[\frac{(5.6146)(100E9)(.000686)}{(3.1416)(30)(.25)(1)(.75)} \right]^{0.5} = 4668.27 \text{ ft.}$$

2. Calculate G_p . for a fixed time increment of 91.25 days.

$$G_p = 91.25 * 30E6 = 2.7375 \text{ BCF}$$

3. Estimate pressure at original gas water contact, P_{rg} .

$$P_{rg} = 4820 \text{ psia}$$

4. Solve eq. 5 for W_e aquifer.

$$\begin{aligned} B &= (1.1191) (.25) (9E-6) (30) (4668.27)^2 (1) \\ &= 1646.21 \text{ bbl/psia.} \end{aligned}$$

$$\Delta P = (5000 - 4820)/2 = 90 \text{ psia}$$

$$t_D = \frac{(.006323) (500) (91.25)}{(.25) (.7) (9E-6) (4668.27)^2} = 8.405$$

From the $R_a/R_g = 10$ curve of dimensionless influx unit, W_{eD} , find corresponding to $t_D = 8.405$.

$$W_{eD} = 6.539$$

$$\begin{aligned} W_e \text{ aq.} &= 1646.21 * 90 * 6.539 \\ &= 968,811 \text{ bbl.} \end{aligned}$$

5. Calculate the radius of the univaded zone, R_c , by solving eq. 9.

$$\begin{aligned} R_c &= \left[(4668.27)^2 - \frac{5.6146 * 968,811}{(1-.35-.25) * 3.1416 * .25 * 30 * 1} \right]^{0.5} \\ &= 4613 \text{ ft} \end{aligned}$$

6. Calculate the pressure at the invading water front, P_{rc} , by solving eq. 10.

$$q_w = W_e / t = 968,811 / 91.25 = 10,617 \text{ bbl/day}$$

$$P_{rc} = (4820) - \frac{10,617 * 0.7 * \ln(4668.27 / 4613)}{.00708 * 500 * 30} - 0.433 * 1.02 * \tan 10 * (4668.27 - 4613)$$

$$P_{rc} = 4814.86 \text{ psia}$$

$$B_{gr} = 0.000704 \text{ rb/scf}$$

7. Using eq. 11, calculate the average pressure, P_t , in the water invaded region.

$$P_t = (4820) - \frac{10,617 * 0.7 * \ln(4668.27 / 4613)}{.00708 * 500 * 30} \left[0.5 - \frac{(4613)^2 * \ln(4668.27 / 4613)}{(4668.27)^2 - (4613)^2} \right] - 0.433 * 1.02 * \tan 10 \left[4668.27 - \frac{2}{3} \frac{(4668.27)^2 + (4668.27)(4613) + (4613)^2}{4668.27 + 4613} \right]$$

$$P_t = 4817.85 \text{ psia}$$

$$B_{gt} = 0.000703 \text{ rb/scf}$$

8. Solve eq. 14 and 15 for W_{em} .

$$A = \left[\frac{0.35}{1-.35-.25} \right] \left[\frac{0.000704 - 0.000703}{0.000703} \right] = 0.0011064$$

$$W_{em} = \frac{(100E9 * 0.000686) - (100E9 - 2.7375E9) * 0.000704}{1 - 0.0011064}$$

$$= 127,341 \text{ bbl}$$

9. Compare W_e calculated from step 4 with that calculated from step 8.

$$W_{em} - W_e \text{ aq.} = |127,341 - 969,811| = 842,470 \text{ bbl.}$$

Since $|W_{em} - W_e \text{ aq.}| > 1000$ (tolerance), go to step 3, assume new pressure, and repeat the procedure until the difference between $|W_{em} - W_e \text{ aq.}|$ less than tolerance.

After iterating several times the final pressures and P_{rc}/Z_{rc} were:

$$P_{rg} = 4874.42 \text{ psia}$$

$$P_{rc} = 4868.77 \text{ psia, and}$$

$$P_{rc}/Z_{rc} = 4866.89 \text{ psia}$$

10. Solve eq. 20 for W_e at abandonment condition.

$$W_{ea} = 31.095 \text{ MMbbl}$$

11. Repeat step 3 through 10 for the next time step until G_p equals G or W_{ea} from step 10 greater than W_e either from step 4 or step 8.

APPENDIX B

PROGRAM LISTING

```

C   PERFORMANCE PREDICTION OF WATER DRIVE-GAS RESERVOIR
C   WITHOUT THE INVADED ZONE PRESSURE GRADIENT EFFECT
C   (CONVENTIONAL MATERIAL BALANCE)
C   -----
C   We      = Water influx from aquifer equation.
C   Wem     = Water influx from material balance equation.
C   Qmax    = Max. q-sub-td for appropriate RD (Ra/Rg).
C   fr      = Fraction of perimeter.
C   Ev      = Volumetric sweep efficiency.
C   PIN     = Initial reservoir pressure.
C   NT      = Number of time step
C   DT      = delta time step.
C   POZA    = P/Z at abandonment.
C   -----

      REAL P(0:200),We(0:200),Wem(0:200),POZ(0:200)
      REAL Time(0:200),Kw(3),Qg(5),POZA(0:200),Gp(0:200)

      OPEN (10,FILE = 'REST.OUT',STATUS = 'OLD')
      OPEN (8,FILE = 'DATA.DAT',STATUS = 'OLD')

C   Reading data input

      READ (8,*)DT, RD, Qmax, Sgr, Ev, fr
      READ (8,*)PHI, Uw, SG, Cf, Cw, Swi
      READ (8,*)h, G, PIN, Tres, NT
      READ (8,*)Qg(1), Qg(2), Qg(3), Qg(4), Qg(5)
      READ (8,*)Kw(1), Kw(2), Kw(3)

C   Setting initial conditions

      Gp(0)   = 0.
      We(0)   = 0.
      Wem(0)  = 0.
      P(0)    = PIN
      Time(0) = 0.
      Pk      = PIN
      Ps      = 0.
      NTIME   = -1.

```

```

CALL PSEUDO(PIN,SG,Tres,Pr,Tr)
CALL ZFAC(Pr,Tr,Z,NTIME)
POZ(0) = PIN/Z
POZA(0) = POZ(0)/Vt
Bgi    = .0050346*Tres/POZ(0)
Rgs    = (G*Bg*5.6146)/(fr*PHI*h*3.1416*(1.-Swi))
Ce     = Cf+Cw
B      = 1.1191*PHI*Ce*h*Rgs*fr
Vt     = (1.-Ev)+(Ev*Sgr)/(1.-Swi)

```

C Pressure calculations

```

DO 100 J = 1,3
DELTD = .006323*Kw(J)/(PHI*Uw*Ce*Rgs)
DO 200 I = 1,5
DO 300 N = 1,NT
Time(N) = Time(N-1) + DT
Gp(N)   = Gp(N-1) + (Qg(I)*DT)
IF (Gp(N) .GT. G) GOTO 1000
500 P(N)   = (Pk+Ps)/2.
KI      = N+1
CALL WATRAD(DELTD,N,Qmax,Time,P,KI,W)
We(N)   = B*W
CALL PSEUDO(P(N),SG,Tres,Pr,Tr)
CALL ZFAC(Pr,Tr,Z,NTIME)
POZ(N)  = P(N)/Z
Bg      = .0050346*Tres/POZ(N)
Wem(N)  = (Gp(N)*Bg)-G*(Bg-Bgi)
IF (ABS(Wem(N)-We(N)) .GT. 1000.) THEN
  IF (Wem(N) .GT. We(N)) THEN
    Pk = P(N)
    GOTO 500
  ELSE
    Ps = P(N)
    GOTO 500
  ENDIF
ELSE
  POZA(N) = POZ(0)*(1.-(Gp(N)/G))/Vt
  IF (POZA(N) .LT. POZ(N)) GOTO 1000
ENDIF
Pk = P(N)
Ps = 0.
300 CONTINUE
1000 Pk = PIN
Ps = 0.
Qg(I) = Qg/10**6
WRITE(10,5000) PIN,G,Qg(I),Kw(J),Sgr,Ev,RD

```

```

        WRITE(10,5500)
        DO 1500 L = 0,N
            Gp(L) = Gp(L)/10**9
            We(L) = We(L)/10**6
            WRITE(10,60000)Time(L),Gp(L),P(L),POZ(L)
+           ,POZA(L),We(L)
1500      CONTINUE
200      CONTINUE
100      CONTINUE

```

C Formats

```

5000      FORMAT(15X,'Performance Prediction Without the
+         Gradient Effect',/,23X,'(Conventional Material
+         Balance)',////////,9X,'PI = ',F6.1,' psi',2X,
+         'OGIP = ',F5.1,' BCF',2X,'Qg = ',F4.1,
+         ' MMBBL',2X,'Kw = ',F5.1,' md',/,20X,
+         'Sgr = ',F4.2,4X,'Ev = ',F4.2,4X,'Ra/Rg = ',
+         F4.1,////)
5500      FORMAT(8X,' TIME           Gp           PRESSURE           POZ'
+         '           POZA           CUM We',/,
+         8X,' (DAYS)           BCF           (PSI)           (PSI)'
+         '           (PSI)           MMBBL',/,
+         8x,'-----           -----           -----           -----'
+         '           -----           -----',/))
6000      FORMAT(8X,F7.2,2X,F7.3,2(2X,F7.2),3X,F8.2,5X,F7.3)
STOP
END

```

```

C   PERFORMANCE PREDICTION OF WATER-DRIVE GAS RESERVOIR
C   WITH THE INVADDED ZONE PRESSURE GRADIENT EFFECT
C   (MODIFIED MATERIAL BALANCE)

```

```

C -----
C   deg   = Dip angle.
C   Prg   = Pressure at OGWC
C   Prc   = Pressure at CGWC
C   Pt    = Average pressure at water-invaded zone
C -----

```

```

REAL Prg(0:200), We(0:200), Wem(0:200), Kwg, Krw
REAL Time(0:200), Kw(3), Qg(5), POZA(0:200)
REAL Prc(0:200), Gp(0:200)
OPEN (10, FILE = 'REST.OUT', STATUS = 'OLD')
OPEN (8, FILE = 'DATA.DAT', STATUS = 'OLD')

```

```

C   Reading data input

```

```

READ (8, *) DT, RD, Sgr, Ev, fr, Rho
READ (8, *) PHI, Uw, SG, Cf, Cw, Swi
READ (8, *) h, G, PIN, Tres, NT, Qmax
READ (8, *) Qg(1), Qg(2), Qg(3), Qg(4), Qg(5)
READ (8, *) Kw(1), Kw(2), Kw(3)

```

```

C   Setting initial conditions

```

```

Gp(0)   = 0.
We(0)   = 0.
Wem(0)  = 0.
Prg(0)  = PIN
Prc(0)  = pin
Time(0) = 0.
Pk      = PIN
Ps      = 0.
NTIME   = -1.
CALL PSEUDO(PIN, SG, Tres, Pr, Tr)
CALL ZFAC(Pr, Tr, Z, NTIME)
POZ(0)  = PIN/Z
POZA(0) = POZ(0)/Vt
Bgi     = .0050346*Tres/POZ(0)
Rgs    = (G*Bgi*5.6146/(fr*PHI*h*3.1416*(1.-Swi)))
Rg     = SQRT(Rgs)
Ce     = Cf+Cw
B      = 1.1191*PHI*Ce*h*Rgs*fr
Vt     = (1.-Ev)+(Ev*Sgr)/(1.-Swi)
Wea    = G*Bgi*(1.-Vt)
Const1 = (1.-Sgr-Swi)*PHI*Uw*h*3.1416*fr

```

```

Const2 = Sgr/(1.-Sgr-Swi)
Const3 = .433*Rho*TAN(DEG*3.1416/180.)
Krw = SQRT((1.-Sgr-Swi)/(1.-Swi))*(1.-Sgr)**3

```

C Pressure calculations

```

DO 100 J = 1,3
  Kwg = Krw*Kw(J)
  DELTD = .006323*Kw(J)/(PHI*Uw*Ce*Rgs)
  FACT1 = Uw/.00708/Kwg/h
  DO 200 I = 1,5
    DO 300 N = 1,NT
      Time(N) = Time(N-1) + DT
      Gp(N) = Gp(N-1) + (Qg(I)*DT)
      IF (Gp(N) .GT. G) GOTO 1000
500   Prg(N) = (Pk+Ps)/2.
      KI = N+1
      CALL WATRAD(DELTD,N,Qmax,Time,Prg,KI,W)
      We(N) = B*W
      Qw = (We(N)-We(N-1))/(Time(N)-Time(N-1))
      Rcs = Rgs-(5.6146*We(N)/Const1)
      IF (Rcs .LT. 0) THEN
        Ps = Prg(N)
        GOTO 500
      ELSE
        Rc = SQRT(Rcs)
      ENDIF
      DP1 = Qw*LOG(Rg/Rc)*FACT1
      DP2 = Const3*(Rg-Rc)
      Prc(N) = Prg(N)-DP1-DP2
      IF (Prc(N) .LE. 0) THEN
        Ps = Prg(N)
        GOTO 500
      ELSE
        CALL PSEUDO(Prc(N),SG,Tres,Pr,Tr)
        CALL ZFAC(Pr,Tr,Z,NTIME)
        POZ(N) = Prc(N)/Z
        Bgr = .0050346*Tres/POZ(N)
      ENDIF
      FACT2 = Rcs*LOG(Rg/Rc)/(Rgs-Rcs)
      FACT3 = (Rgs+Rcs+Rc*Rg)/(Rg+Rc)
      Pt = Prg(N)-Qw*FACT1(.5-FACT2)-Const3*
+      (Rg-(2.*FACT3/3.))
      CALL PSEUDO(Pt,SG,Tres,Pr,Tr)
      CALL ZFAC(Pr,Tr,Z,NTIME)
      Bgt = .0050346*Tres*Z/Pt
      FACT4 = 1.-CONST2*(Bgr-Bgt)/Bgt

```

```

Wem(N) = (G*Bgi-(G-Gp(N))Bgr)/FACT4
IF (ABS(Wem(N)-We(N)) .GT. 1000.) THEN
  IF (Wem(N) .GT. We(N)) THEN
    Pk = Prg(N)
    GOTO 500
  ELSE
    Ps = Prg(N)
    GOTO 500
  ENDIF
ELSE
  IF (Wea .LT. We(N)) GOTO 1000
ENDIF
Pk = Prg(N)
Ps = 0.
300 CONTINUE
1000 Pk = PIN
    Ps = 0.
    Qg(I) = Qg/10**6
    WRITE(10,5000) PIN,G,Qg(I)
    WRITE(10,5100) Kw(J),Kwg,Sgr,Ev
    WRITE(10,5200) RD,deg,Wea
    WRITE(10,5500)
    DO 1500 L = 0,N
      Gp(L) = Gp(L)/10**9
      We(L) = We(L)/10**6
      WRITE(10,60000) Time(L),Gp(L),Prg(L),Prc(L)
      ,POZ(L),We(L)
    +
1500 CONTINUE
200 CONTINUE
100 CONTINUE

```

C Formats

```

5000 FORMAT(15X,'Performance Prediction With the
+ Gradient Effect',/,23X,'(Modified Material
+ Balance)',/,13X,'PI = ',F6.1,' psi',2X,'
+ OGIP = ',F5.1,' BCF',2X,'Qg = ',F4.1,'
+ MMBBL',/)
5100 FORMAT(12X,'Kw = ',F5.1,' md',2X,'Kwg = ',F5.1,
+ ' md',',Sgr = ',F4.2,4X,'Ev = ',F4.2,/)
5200 FORMAT(11X,'Ra/Rg = ',F4.1,' Dip Angle = ',F4.1,
+ 'Wea = ',F7.3,' MMBBL',/)
5500 FORMAT(8X,' TIME Gp Prg Prc'
+ ' POZ CUM We',/,
+ 8X,' (DAYS) BCF (PSI) (PSI)'
+ ' (PSI) MMBBL',/,
+ 8X,'-----'
+ '-----',/)

```

```
6000  FORMAT(8X,F7.2,2X,F7.3,2(2X,F7.2),3X,F8.2,5X,F7.3)
      STOP
      END
```

CSM Program Library
water influx subroutine

REFERENCE NUMBER: PE:SR009.FOR.JDW

TITLE: WATRAD.FOR

AUTHOR: j d wright

DATE: 10-DEC-74

SOURCE LANGUAGE: FORTRAN-10

DESCRIPTION: this subroutine calculates water influx based on curves fitted to the tables presented by van everdingen and hurst. this subroutine follows the unsteady state curve until the q -sub- td calculated is greater than the $qtdmax$ specified in the call statement. this has the effect of ignoring the transition from unsteady state to pseudo steady state flow. the user must provide an array of time and an array of the corresponding pressures dimensioned from zero to whatever the maximum number of time step is.

CALL WATRAD(DELTD,N,QTDMAX,TIME,P,K,WFLUX)

DELTD = INPUT: delta dimensionless time.
N = INPUT: time of interest. you want to solve for the cumulative water influx at this time. (this is the location of the time of interest in the time array.) remember that the initial time and pressure are stored in the zero location in the same time and p arrays.
QTDMAX = INPUT: for finite reservoirs this is the maximum q -sub- td that they can provide. for an infinite reservoir set $qtdmax$ to zero or negative number.
TIME = INPUT: an array (from 0 to k) containing the various time.
P = INPUT: an array (from 0 to k) containing the various pressures corresponding to the above time.

K = INPUT: the size of the time and p arrays.
WFLUX = OUTPUT: the summation of q -sub- t d times
delta p from time=0 to time= n . must
be multiplied by 'b' (the water
influx coefficient) to get cumulative
water influx at time n .

SUBPROGRAMS USED: none

REFERENCES: craft and hawkins, page 221. van everdingen,
timmerman, and mcMahon, 'application of the material
balance equation to a partial water drive reservoir',
petroleum transactions, aime, vol 198, 1953, page 51.

(Adapted from "PELIB:WATRAD.MEM", CSM Program Library with
permission of the author.)

CSM Program Library
z-factor subroutine

REFERENCE NUMBER: PE:SR001.F4.JDW

TITLE: ZFAC.F4

AUTHOR: j d wright

DATE: 29-OCT-74

SOURCE LANGUAGE: FORTRAN-40

DESCRIPTION: this subroutine calculates the compressibility factor of a mixture of natural gases. the method is a table lookup and interpolation on a table of 400 z-factors. 4-point lagrange interpolation is used on pseudo reduced pressure and either 4-point lagrange or linear interpolation is on reduced temperature.

the limits on reduced pressure are zero to 15. the limits on reduced temperature are 1.05 to 3.00.

CALL ZFAC(PR,TR,Z,NTIME)

PR = INPUT: pseudo reduced pressure.
TR = INPUT: pseudo reduced temperature.
Z = OUTPUT: z-factor. set to zero if pr or tr out of range.
NTIME = INPUT: call to rtime can be disabled by supplying a negative number for ntime when the subroutine is called. this will save quite a bit of time since two calls to rtime are made in zfac.
OUTPUT: cpu time of this call to zfac in millisec. usually should be disabled as shown above.

SUBPROGRAMS USED: fx- lagrange interpolation subroutine.

REFERENCES: gray and simms, oil and gas journal, july 20, 1959, vol 57, no 30.

(Adapted from "PELIB:ZFAC.MEM", CSM Program Library with permission of the author.)

CSM Program Library
pseudo reduced properties

REFERENCE NUMBER: PE:SR002.F4.JDW

TITLE: PSEUDO.F4

AUTHOR: j d wright

DATE: 29-OCT-74

SOURCE LANGUAGE: FORTRAN-40

DESCRIPTION: this subroutine calculates the pseudo reduced pressure and the pseudo reduced temperature of a mixture of natural gases. the acceptable range of gas gravity is .55 to 1.2.

CALL PSEUDO(P,G,TRANK,PR,TR)

P = INPUT: pressure, psia
G = INPUT: gas gravity (air = 1)
TRANK = INPUT: temperature, deg rankine
PR = OUTPUT: pseudo reduced pressure.
TR = OUTPUT: pseudo reduced temperature.

SUBPROGRAMS USED: none.

REFERENCES: amyx, bass, and whiting, page 259 - misc gases.

(Adapted from "PELIB:PSEUDO.MEM" CSM Program Library with permission of the author.)

TABLE B-1

Performance Prediction Without the Gradient Effect
(Conventional Material Balance)

Pi = 5000 psia OGIP = 100 BCF Qg = 30 MMCFD Kw = 500 md

Sgr = 0.35 Ev = 0.85 Ra/Rg = 10.0

TIME (DAYS)	Gp BCF	PRESSURE (PSIA)	POZ (PSIA)	POZA (PSIA)	CUM We MMBBL
0.00	0.000	5000.00	4594.53	9063.16	0.000
91.25	2.737	4870.76	4868.24	8815.06	0.696
182.50	5.475	4819.48	4833.32	8566.95	2.130
273.75	8.212	4778.44	4805.12	8318.85	3.675
365.00	10.950	4747.82	4783.91	8070.75	5.332
456.25	13.688	4723.91	4767.24	7822.64	7.062
547.50	16.425	4704.31	4753.51	7574.54	8.843
638.75	19.162	4688.23	4742.21	7326.43	10.661
730.00	21.900	4674.50	4732.54	7078.33	12.508
821.25	24.637	4662.51	4724.07	6830.23	14.377
912.50	27.375	4651.98	4716.59	6582.12	16.264
1003.75	30.112	4742.62	4709.94	6334.02	18.165
1095.00	32.850	4634.11	4703.89	6085.91	20.079
1186.25	35.587	4626.62	4698.55	5837.81	22.002
1277.50	38.325	4619.42	4693.41	5589.70	23.934
1368.75	41.063	4590.66	4672.79	5341.60	25.728
1460.00	43.800	4544.01	4639.07	5093.50	27.422
1551.25	46.537	4503.38	4609.43	4845.39	29.175
1642.50	49.275	4465.31	4581.42	4597.29	30.965
1733.75	52.013	4431.52	4556.35	4349.19	32.799

TABLE B-2

Performance Prediction With the Gradient Effect
(Modified Material Balance)

Pi = 5000 psia OGIP = 100 BCF Qg = 30 MCFD

Kw = 500 md Kwg = 100.3 Sgr = 0.35 Ev = 0.85
Ra/Rg = 10.0 Dip Angle = 10 Wea = 31.095 MMBBL

TIME (DAYS)	Gp BCF	Prg (PSIA)	Prc (PSIA)	POZ (PSIA)	CUM We MMBBL
0.00	0.000	5000.00	5000.00	4954.53	0.000
91.25	2.737	4874.42	4868.77	4866.89	0.676
182.50	5.475	4832.40	4808.31	4825.68	2.027
273.75	8.212	4795.38	4752.63	4787.25	3.443
365.00	10.950	4769.85	4704.47	4753.85	4.954
456.25	13.688	4749.18	4660.02	4722.31	6.516
547.50	16.425	4732.51	4617.11	4691.76	8.120
638.75	19.162	4718.43	4574.86	4661.41	9.756
730.00	21.900	4706.19	4532.28	4630.54	11.417
821.25	24.637	4695.42	4488.84	4598.76	13.099
912.50	27.375	4685.53	4443.60	4565.33	14.801
1003.75	30.112	4676.45	4396.00	4529.82	16.521
1095.00	32.850	4668.04	4345.49	4491.71	18.258
1186.25	35.587	4659.92	4290.81	4450.00	20.132
1277.50	38.325	4652.17	4231.01	4403.80	21.785
1368.75	41.063	4615.54	4157.96	4346.54	23.471
1460.00	43.800	4570.46	4069.03	4275.59	25.107
1551.25	46.537	4536.71	3966.63	4192.20	26.773
1642.50	49.275	4500.44	3849.92	4094.88	28.463
1733.75	52.013	4469.95	3709.49	3974.51	30.207
1825.00	54.750	4438.44	3530.21	3815.56	32.005